LA-UR-22-33109

Approved for public release; distribution is unlimited.

Title:	Neptunium (V) Solubility in the Presence and Absence of WIPP Relevant Ligands
Author(s):	Kaplan, Ugras
Intended for:	Report
Issued:	2022-12-21

LOS ALAMOS NATIONAL LABORATORY
CARLSBAD OPERATIONS

LCO-ACP-30, Rev 0

Neptunium (V) Solubility in the Presence and Absence of WIPP Relevant Ligands

Effective Date: 12-22-22

Originator:

Ugras Kaplan, LANL-CO ACRSP — Date: 12/21/2022

Reviewed by:

Ceren Kutahyali Aslani, LANL-CO ACRSP — Date: 12/21/2022

Approved by:

Jeremiah Beam, LANL-CO ACRSP, Team Leader — Date: 12/21/2022

Priscilla Yanez, LANL-CO Quality Assurance Manager — Date: 12/21/2022

Douglas Weaver, WIPP/RSO Program Director — Date: 12-21-2022

History of Revision/Change

Revision Number	Effective Date	Pages Affected	Description of Revision
0		All	Original Release

TABLE OF CONTENTS

LIST OF TABLES

LIST OF FIGURES

EXECUTIVE SUMMARY

CRA (Compliance Recertification Application)-2024 will update the oxidation state specific model used to calculate actinide solubility in the WIPP (Waste Isolation Pilot Plant). The pentavalent Np(V) ion is the most stable ion in solution within the An(V) series. This valence stability of Np(V) in aqueous solution makes Np a useful representative element for studying the aqueous complex chemistry of all An(V), but in the predicted WIPP scenario, this is the only TRU component that increases in the inventory with time as it is the main daughter product of ^{241}Am decay (alpha, n) so its relative importance increases throughout the 10,000-year performance period of the WIPP, it is only used to represent itself. This work is focused on confirming organic, borate and carbonate effects on solubility of Np(V) in WIPP simulated brines and 5 M NaCl and reassessing the predicted model speciation to strengthen the overall WIPP An(V) model.

The aqueous chemistry of Np(V) in 5 M NaCl and synthetic WIPP brines as a function of pC_{H+} in presence and absence of borate, WIPP relevant ligands (EDTA, oxalate, citrate, acetate) and carbonate at T = 23 ± 2 °C was thoroughly studied by long-term batch solubility experiments (approximately 150 days) from an undersaturation approach. Applying a comprehensive set of experimental and spectroscopic techniques including UV-VIS-NIR and Np L_{III}-edge X-ray Absorption Spectroscopy (XAS), the solubility controlling Np(V) solid phases and the predominant aqueous Np(V) species were identified in all studying samples. Also, the impact of borate on the aqueous speciation and especially on the solubility of Np(V) in 5 M NaCl and synthetic WIPP brines at $pC_{H+} \approx 9$ was confirmed. The interactions of organic ligands with Np(V) vary depending on kinetics. It was observed that acetate increased the neptunium solubility within the 150-days experimental period, and this result confirms the WIPP model prediction. The effect of carbonate on Np(V) solubility is mostly seen at pC_{H+} 7 and pC_{H+} 11.

The data obtained from this work quantify the effects of WIPP-relevant concentrations of organics/borate/carbonate on the solubility of Np(V) to challenge the predictions of the WIPP actinide model and inform decisions and recommendations made in the upcoming recertification of the WIPP (CRA-2024).

The experiments were performed by the Los Alamos National Laboratory-Carlsbad Operations (LANL-CO) Actinide Chemistry and Repository Science Program (ACRSP) as part of a larger effort to establish the conservatisms related to actinide chemistry in the current WIPP Performance Assessment (PA) model, and establish a more robust WIPP chemistry conceptual model to support ongoing WIPP recertification efforts. The experiments were performed under the United State Department of Energy (US DOE) approved test plan "Experimental Strategy to Challenge Actinide Solubility Predictions" LCO-ACP-26. All data reported were generated under the Los Alamos National Laboratory−Carlsbad Operations (LANL-CO) WIPP Quality Assurance (QA) Program,

which is compliant with the DOE Carlsbad Field Office (CBFO) Quality Assurance Program Document (QAPD) [QAPD 2017].

1. PURPOSE

In CRA-2005, 2009 and 2014, the DOE argued that the potential contributions of Np (V) to release from WIPP could be ignored due to its low inventory. Np is present as the ^{237}Np isotope (half-life = 2.144 $\times 10^6$ year), and its inventory (50 kg in 2033) is expected to increase with time, from the decay of ^{241}Am and possible ^{238}U (n, 2n) reactions, to 331 kg at 1000 years after closure. Other isotopes of Np will be present only at relatively trace levels, ~ 2 mg of ^{239}Np is expected at closure, and will not be associated with analogous increases in mass. CRA-2024 will decide the oxidation state specific model used to calculate actinide solubility in the WIPP.

2. Quality Assurance, References, Acronyms, and Definitions Quality

This work was compliant with the LANL-CO-QA program. All experimental procedures and data analysis are included in scientific notebook ACP-26-3, issued to Ugras Kaplan as a "Test Plan LCO-ACP-26, rev. 1 Task 3: Experimental Plans/Approach to Challenge the An(V) WIPP Model". Data collection was performed as outlined in QA approved procedures. Descriptions of the experiments can be found in the scientific notebook designated ACP-26-03.

2.1.References

[ACP-EXP-001]: Revision 3 –Brine preparation.

[Altmaier 2003]: M.Altmaier, V.Metz, V.Neck, R.Müller, Th.Fanghänel, Solid-liquid equilibria of $Mg(OH)_{2(cr)}$ and $Mg_2(OH)_3Cl{\cdot}_4H_2O_{(cr)}$ in the system Mg-Na-H-OH-Cl-H_2O at 25°C

[Borkowski 2009]: Borkowski, M., Lucchini, J.-F., Richmann,, M. K. & Reed, D. T. Actinide (III) Solubility in WIPP Brine: Data Summary and Recommendations, s.l.: Los Alamos National Laboratory; Carlsbad, NM. LA-UR-10-14360, (2009).

[Borkowski 2010]: Borkowski, M., M.K. Richmann, D.T. Reed, and Y.-L. Xiong. Complexation of Nd(III) with Tetraborate Ion and Its Effect on Actinide(III) Solubility in WIPP Brine. Radiochimica Acta. 98.9-11 (2010): 577–582, (2010).

[Brendebach 1980]: Brendebach, B., Banik, N. L., Marquardt, Ch. M., Rothe, M., Denecke, M. A., Geckeis, H., X-ray absorption spectroscopic study of trivalent and tetravalent actinides in solutions at varying pH values, Radiochim. Acta, 97, 701–708 (2009).

[Buda 2008]: Buda, R. A.; Banik, N. L.; Kratz, J. V.; Trautmann, N. Studies of the ternary systems humic substances - kaolinite - Pu(III) and Pu(IV) Radiochim. Acta, 96 (9–11) 657–665 DOI: 10.1524/ract.2008.1550 (2008).

[Bynaum 1999]: Bynaum, R V, Free, S J, and Moore, R C. A Thermodynamic Model for Acetate, Lactate, and Oxalate Complexation with Am(III), Th(IV), Np(V), and U(VI) Valid to High Ionic Strength. United States: N. p., (1999).

[Choppin 2001]: Choppin, G.R., A.H. Bond, M. Borkowski, M.G. Bronikowski, J.F. Chen, S. Lis, J. Mizera, O. Pokrovsky, N.A. Wall, Y.X. Xia, and R.C. Moore. Waste Isolation Pilot Plant Actinide Source Term Test Program: Solubility Studies and Development of Modeling Parameters. SAND99-0943. ERMS 518556. Albuquerque: Sandia National Laboratories (2001).

[Choppin 2007]: Choppin, G. R. Actinide speciation in the environment J. Radioanal. Nucl. Chem, 273 (3) 695– 703 DOI: 10.1007/s10967-007-0933-3, (2007).

[CRA 2014]: DOE (U.S. Department of Energy), 2014. Title 40 CFR Part 191 Subparts B and C Compliance Recertification Application for the Waste Isolation Pilot Plant. U.S. Department of Energy Carlsbad Field Office, March (2014) Retrieved from https://www.wipp.energy.gov/library/CRA/CRA-2014.html

[Domski and Sisk-Scott 2019]: Domski, P.S., and C. Sisk-Scott. Prediction of Baseline Actinide Solubilities for CRA-2019 with an Updated EQ3/6 Pitzer Thermodynamic Database, DATA0.FM4. Sandia National Laboratories Report. ERMS 571178 (2019).

[Fanghänel 1995]: Fanghänel, Th., Neck, V., Kim, J. I.: "Thermodynamics of Neptunium(V) in Concentrated Salt Solutions: II. Ion Interaction (Pitzer) Parameters for Np(V) Hydrolysis Species and Carbonate Complexes." Radiochim. Acta 69, 169—176 (1995).

[Fellhauer 2016]: David Fellhauer*, Jörg Rothe, Marcus Altmaier, Volker Neck, Jörg Runke, Thierry Wiss, and Thomas Fanghänel, Th., Np(V) solubility, speciation and solid phase formation in alkaline CaCl2 solutions. Part I: Experimental results, Radiochim. Acta; 104(6): 381–397, (2016).

[Gaona 2012]: Gaona, X., Tits, J., Dardenne, K., Liu, X., Denecke, M. A., Wieland, E., Altmaier, M., Spectroscopic investigations of the Np(V/VI) redox speciation in hyperalkaline TMA-(OH, Cl) solutions, Radiochim. Acta 100, 759–770 (2012).

[Giambalvo 2002]: Giambalvo, E.R. 2002. Memorandum to L.H. Brush. Subject: Recommended Parameter Values for Modeling An(V) Solubility in WIPP Brines. 26 July 2002. Carlsbad, NM: Sandia National Laboratories. ERMS 522990, (2002).

[Hinz 2015]: K. Hinz, M. Altmaier, X. Gaona, T. Rabung, D. Schild, M. Richmann, D. T. Reed, E. V. Alekseev and H. Geckeis, New J. Chem., 39, 849–859, (2015).

[Hinz 2020]: K. Hinz a, D. Fellhauer a, X. Gaona , M. Vespa, K. Dardenne, D. Schild O, T. Yokosawa, M. A. Silver, D. T. Reed , T. E. Albrecht-Schmitt, M. Altmaier a and H. Geckeis. Interaction of Np(V) with borate in alkaline, diluteto-concentrated, NaCl and MgCl2 solutions; Cite this: Dalton Trans. 49,1570, (2020).

[INV-PA-18, 2018]: Performance Assessment Inventory Report, Revision 0 - 2018

[Kaszuba 1999]: J. P. Kaszuba and W. H. Runde, “The aqueous geochemistry of neptunium: Dynamic control of soluble concentrations with applications to nuclear waste disposal”, Environ. Sci. Technol., 33, 4427 (1999).

[Kim 2006]: J. I. Kim, “Significance of actinide chemistry for the longterm safety of waste disposal”, Nucl. Eng. Technol., 38, 459 (2006).

[Kropf 2010]: Kropf, A.J., et al. The New MRCAT (Sector 10) Bending Magnet Beamline at the Advanced Photon Source. In AIP Conference Proceedings, vol. 1234, no. 1, pp. 299-302. American Institute of Physics, (2010).

[Kropf 2010]: Kropf, A.J., et al. The New MRCAT (Sector 10) Bending Magnet Beamline at the Advanced Photon Source. In AIP Conference Proceedings, vol. 1234, no. 1, pp. 299-302. American Institute of Physics, (2010).

[LCO-ACP-08]: Actinide (III) Solubility in WIPP Brine: Data Summary and Recommendations (2009).

[LCO-ACP-26]: Experimental Strategy to Challenge Actinide Solubility Predictions (2021)

[Lierse 1985]: C. Lierse, W. Treiber, and J. I. Kim, "Hydrolysis reactions of Neptunium(V)", Radiochim. Acta., 38, 27 (1985).

[Mahamid 1998]: I. A. Mahamid, C.F. Novak, K.A Becraft, S. A. Carpenter, and N. Hakem, "Solubility of Np(V) in K-Cl-CO3 and Na- K-Cl-CO3 Solutions to High Concentrations: Measurements and Thermodynamic Model Predictions", Radiochim. Acta., 81, 93 (1998).

[Maiwald 2018]: Martin M. Maiwald; Thomas Sittel; David Fellhauer; Andrej Skerencak-Frech; Petra J. Panak, The Journal of Chemical Thermodynamics, ISSN: 0021-9614, 1018, Vol: 116, Page: 309-315, (2018).

[Neck 1994]: Neck, V., Runde, W., Kim, J. I., Kanellakopulos, B.: Solid-Liquid Equilibrium Reactions of Neptunium(V) in Carbonate Solution at Different Ionic Strength. Radiochim. Acta 65, 29 (1994).

[Neck 1995a]: V. Neck, W. Runde, and J. I. Kim, "Solid-liquid equilibria of neptunium(V) in carbonate solutions of different ionic strengths: II. Stability of the solid phases", J. Alloys Comp., 225, 295 (1995).

[Neck 1995b]: Neck, V., Fanghänel, T., Rudolph, G., Kim, J. I.: Thermodynamics of neptunium(V) in concentrated salt-solutions complexation and ion-interaction (Pitzer) parameters for the NpO_2^+ ion. Radiochim. Acta 69, 39 (1995).

[Neck 1995c]: Neck, V., Fanghänel, Th., Kim, J. I.: Dissoziationskonstanten von H_20 und H_2C0_3 in $NaClO_4$-Lösung und Pitzer-Para-meter im System $Na^+/H^+/OH^-$

/HC0l/C0r/C10j/H20, 25 °C, Report FZKA 5599, Forschungszentrum Karlsruhe, (1995).

[Nitsche 1992]: Nitsche H., Müller A., Standifer E. M., Deinhammer R. S., Becraft K., Prussin T., and Gatti R. C.; Dependence of Actinide Solubility and Speciation on Carbonate Concentration and Ionic Strength in Groundwater; Radiochimica Acta 58/59, 2 7 - 3 2 (1992).

[Novak 1996]: C. F. Novak , H. Nitsche , H. B. Silber , K. Roberts , Ph. C. Torretto , T. Prussin , K. Becraft , S. A. Carpenter , D. E. Hobart and I. AlMahamid, Neptunium(Y) and Neptunium(VI) Solubilities in Synthetic Brines of Interest to the Waste Isolation Pilot Plant (WIPP), Radiochimica Acta 74, 31-36 (1996).

[Novak 1997]: C. F. Novak, I. Al Mahamid, K. A. Becraft, S. A. Carpenter, N. Hakem, and T. Prussin, "Measurement and Thermodynamic Modeling of Np(V) Solubility in Aqueous K2CO3 Solutions to High Concentrations", J. Sol. Chem., 26, 681 (1997).

[Petrov 2017]: Vladimir G. Petrov, David Fellhauer, Xavier Gaona, Kathy Dardenne, Jörg Rothe, Stepan N. Kalmykov and Marcus Altmaier Solubility and hydrolysis of Np(V) in dilute to concentrated alkaline NaCl solutions: formation of Na–Np(V)–OH solid phases at 22 °C, Radiochim. Acta; 105(1): 1–20, (2017).

[Pokrovsky 1997]: Pokrovsky, O. S,, Bronikowski, M. G,, Moore, R. C., Choppin, G. R.: Neptunium(V) Complexation by Acetate, Oxalate and Citrate in NaC104 Media at 25°C. Radiochimica Acta 79, 167-171 (1997).

[QAPD 2017]: QAPD, 2017. QUALITY ASSURANCE PROGRAM DOCUMENT, s.l. : DOE/CBFO-94-1012.

[Ravel 2005]: Ravel, B.; Newville, M. ATHENA, ARTEMIS, HEPHAESTUS: data analysis for X-ray absorption spectroscopy using IFEFFIT J. Synchrotron Radiat, 12, 537– 541 DOI: 10.1107/S0909049505012719, (2005).

[Reed 1998]: Reed, D.T., S.B. Aase, D. Wygmans, and J. E. Banaszak. "The Reduction of Np(VI) and Pu(VI) by Organic Chelating Agents." Radiochimica Acta, vol. 82: 109-14, (1998).

[Runde 2000]: Runde W.; Chemical Interactions of Actinides in the Environment, Los Alamos Science Number 26 (2000).

[Runde 2002]: Runde, W.; Conradson, S. D.; Wes Efurd, D.; Lu, N. P.; VanPelt, C. E.; Tait, C. D. Solubility and sorption of redox-sensitive radionuclides (Np, Pu) in J-13 water from the Yucca Mountain site: comparison between experiment and theory Appl. Geochem, 17 (6) 837– 853 DOI: 10.1016/S0883-2927(02)00043-4 (2002).

[Schramke 2020]: Schramke JA, Santillan EFU, Peake RT. Plutonium Oxidation States in the Waste Isolation Pilot Plant Repository. Appl Geochem. 2020 May; 116:10.1016/j.apgeochem. 104561. doi: 10.1016/j.apgeochem.2020.104561. PMID: 32489229; PMCID: PMC7266098, (2020).

[Shilov 2012]: Shilov, V. P., Gogolev, A. V., Fedoseev, A. M., Speciation, stability, and reactions of Np(III–VII) in aqueous solutions, Radiochemistry 54, 212–227 (2012).

[Shott 2015]: J. Schott, J. Kretzschmar, S. Tsushima, B. Drobot, M. Acker, A. Barkleit, S. Taut, V. Brendler and T. Stumpf, Dalton Trans. 44, 11095–11108 (2015).

[SOTERM 2019]: U.S. Department of Energy (DOE). 2019b. Title 40 CFR Part 191 Subparts B and C Compliance Recertification Application 2019, Appendix SOTERM. Carlsbad Field Office, Carlsbad, NM.

2.2.Acronyms and Definitions

ACRONYM	DEFINITION
^{241}Am	Americium 241
Ac.	Acetate: CH_3COOH
ACRSP	Actinide Chemistry and Repository Science Program
am	amorphous solid
An	Generic Actinide
An(III)	Trivalent actinide
An(IV)	Tetravalent actinide
An(V)	Pentavalent actinide
An(VI)	Hexavalent actinide
ANL	Argonne National Laboratory
APS	Advance Photon Source
aq	Aqueous
$[B(OH)_4]^-$	Tetrahydroxyborate
CO_2	Carbon dioxide
Ca	Calcium
$CaCl_2$	Calcium chloride
CBFO	Carlsbad Field Office (U.S. Department of Energy)
Cl^-	Chlorine
Cit.	Citrate: $C_6H_8O_7$
Cm(III)	Trivalent Curium
CO_3^{2-}	Carbonate
CPR	Cellulosic, Plastic, and Rubber materials
cr	Crystalline
CRA	Compliance Recertification Application
DEO	Department of Energy
ε	Molar Absorption Coefficient ($M^{-1}\cdot cm^{-1}$)
EDTA	Ethylenediaminetetraacetic acid: $C_{10}H_{16}N_2O_8$
EQ3/6	Software program for geochemical modeling of aqueous systems
ERDA-6	U.S. Energy Research and Development Administration Well 6, a synthetic brine representative of fluids in Castile brine reservoirs
Eu(III)	Trivalent Europium
eV	Electron volt
Fe(II)	Divalent iron
Ge	Germanium
GWB	Generic Weep Brine, a synthetic brine representative of intergranular Salado-Formation brines

H^+	Hydronium
HBr	Hydrogen Bromide
H_2O	Water
HBr	Hydrogen bromide
HCO_3^-	Bicarbonate
HNO_3	Nitric acid
I_{tot}	Total ionic strength
kDa	Kilodalton
kg	Kilogram
LANL-CO	Los Alamos National Laboratory−Carlsbad Operations
LCFA	Linear Combination Fit Analysis
M	Molarity, moles of solute per liter of solvent
$MgCl_2$	Magnesium chloride
mg	Milligram
mL	Mililiter
Mg	Magnesium
$MgCO_3^-$	Magnesium carbonate
MgO	Magnesium oxide
mM	Mili Molar
Na^+	Sodium ion
$NaC10_4$	Sodium perchlorate
NaCl	Sodium chloride
$NaHCO_3$	Sodium hydrogen carbonate
Nd(III)	Trivalent Neodymium
nm	Nano meter
Np(III)	Trivalent Neptunium ion
Np(IV)	Tetravalent Neptunium ion
Np(V)	Pentavalent Neptunium ion
Np(VI)	Hexavalent Neptunium ion
OH^-	Hydroxide ion
Ox.	Oxalate: $H_2C_2O_4$
PA	Performance Assessment
pC_{H+}	Negative logarithm of H^+ concentration in moles/liter
pH	Negative logarithm of H^+ activity
pH_{exp}	The experimentally measured pH
pH_m	The measured pH
ppm	Parts per million (Microgram/gram)

Pu^{4+}	Tetravalent Plutonium ion
PuO_2^{2+}	Hexavalent Plutonium ion
QAP	Quality Assurance Program
QAPD	Quality Assurance Program Document
RPM	Revolutions per minute
SOTERM	Actinide Source Term (appendix in the WIPP CRA)
SEM-EDS	Scanning electron microscopy (SEM) and energy dispersive
SEM-EDS	X-ray spectroscopy
Si	Silicon
T	Temperature
TRU	Transuranic Element (actinides higher in atomic number than uranium)
US	United States
UV–VIS-NIR	Ultraviolet/Visible/Near Infrared Spectroscopy
WIPP	Waste Isolation Pilot Plant
XAS	X-ray absorption spectroscopy
XANES	X-ray absorption near edge spectroscopy
XPS	X-ray photoelectron spectroscopy
XRD	X-Ray Diffraction
λ_{max}	Maximum wavelength of absorption
Zr	Zirconium

3. Introduction

The Waste Isolation Pilot Plant (WIPP) is the nation's only deep geologic high level radioactive waste repository and also the first operated salt-based deep geologic high level radioactive waste repository in the world. WIPP permanently isolates defense-generated transuranic (TRU) waste 2,150 feet underground in an ancient salt formation [Schramke 2020, CRA 2014]. This radioactive waste needs to be safely disposed to avoid any exposure to humans and the environment.

The breach of the first containment and the resulting release of radionuclides out of the storage canisters and subsequent migration through the enclosing repository corresponds to an accepted and considered incident within safety assessments of waste repositories. The migration of the actinides is determined by different geochemical processes, e.g., redox transformations, colloid formation, sorption/precipitation, desorption/dissolution, solubility and complexation with ligands. This phenomenon is strongly dependent upon composition of the intruding water, geochemistry of the repository waste forms and needs to be properly understood for the long-term performance assessment of a repository for radioactive waste disposal [Choppin 2007, Buda 2008].

Np solubility in WIPP brines which have of high ionic strengths from 5.3 to 7.4 M and alkali pH, is strongly dependent on its oxidation state, with much lower solubilities associated with Np(III) and Np(IV) than with the higher Np(V) and Np(VI) oxidation states [Runde 2000]. Np(IV) is expected to dominate in reducing natural groundwater and Np(V) is expected to be the most common state in more oxidizing waters. The only V actinide of interest to the WIPP is Np(V), which exists as the neptunyl ion, NpO_2^+. The base model for Np(V) comes from, constructed for the German repository program [Fanghänel 1995].

WIPP PA calculations require information on the solubilities of Np(V) in synthetic WIPP brines [Choppin 2001]. However, environmentally relevant neptunium solubility data is concentrated on simple background electrolyte experiments where most existing data were taken in $NaC1O_4$, NaCl, $MgCl_2$ or $CaCl_2$ media [Fellhauer 2016, Neck 1995a, Shilov 2012, Hinz 2020].

Therefore, a well-established and systematic examination of these complicated environmental systems is crucial to describe the chemical behavior of the actinides sufficiently. Before the ternary system actinide/brine component/ligand complexation interaction can be described, the different binary systems, including actinide/brine, actinide/organic ligand and actinide/borate must be investigated. Therefore, present work is divided into three subtasks. These subtasks and literature review will be discussed in the next paragraph in more detail.

Subtask 1: Solubility of Np(V) under WIPP-relevant Conditions

In saline solution, the aqueous Np(V) species are in equilibrium with different solid phases depending on the salt concentration, pH, presence and absence of ligands and CO_2 partial pressure [Neck 1995b, Neck 1994]. The different solubility and interaction behavior of the NpO_2^+ ion in $NaClO_4$, NaCl solutions in the presence and absence of carbonate has been described successfully by considering the interaction between NpO_2^+, Cl^-, ClO_4^- and CO_3^{2-} [Neck 1995b]. Novak et al**.** investigated Np(V) and Np(VI) solubility behavior in WIPP relevant conditions. They claimed that the experimental results would help to determine the applicability of existing Np(V) solubility models, such as the Np(V)-Na-H-Cl-$C1O_4$-HCO_3-CO_3-CO_2(aq)-OH-H_2O model of Fanghänel et al. [Fanghänel 1995], to experiments under WIPP-relevant conditions such as high ionic strength and alkali brine solutions. The Solubility of Np(V) has been measured in three synthetic WIPP simulated Na-K-Mg-Cl Brines in I_{tot}: 0.84, 2.97 and 7.78 respectively in the presence of CO_2(g). An oversaturation experimental approach was performed. Dissolved Np(V) concentrations decreased several orders of magnitude within the first 100 days of the experiment. The solid phases formed in all experiments were identified by X-ray powder diffraction as $KNpO_2CO_3xH_2O_{(S)}$ [Novak 1996].

Subtask 2: Screening Experiments with Organic Complexants to Confirm Model Predictions

Organic ligands affect the speciation of actinides which may form oxidation state specific complexes that can increase the solubility of the oxidation state and stabilize its subsequent reduction or oxidation [Runde 2000]. There are various organic components of nuclear wastes which may be disposal in the WIPP repository. Concentrations of WIPP relevant organics are listed in Table 1 [INV-PA-18, 2018]. The complexation of NpO_2^+ with acetate [Novak 1996], citrate and EDTA [Pokrovsky 1997] and oxalate [Bynaum 1999] in NaCl media have been studied in 5 m (NaCl) ionic strength by a solvent extraction technique.

Table 1. Range in Concentration of Acetate, Oxalate, Citrate and EDTA in the WIPP [INV-PA-18, 2018].

Organic Complexant	Concentration in M
Acetate	2.83×10^{-2}
Oxalate	1.13×10^{-2}
Citrate	2.30×10^{-3}
EDTA	7.92×10^{-5}

In WIPP-specific experiments [Reed 1998], the reduction of Np(VI) to Np(V) in ERDA-6 at pC_{H+} 10 was observed along with complete reduction of Np(VI) to Np(V) in G-Seep (Salado) brine at pC_{H+} 7 when no iron or microbial activity were present. In the presence of oxalate, citrate, and EDTA reduction of Np(VI) to Np(V) reaction complete rapid. At longer times, Np(IV) organic complexes were observed in the presence of citrate. But on the other hand, PuO_2^{2+} was predominantly reduced to Pu^{4+} resulting in the formation of organic complexes or polymeric/hydrolytic precipitates. While the reduction kinetics vary for each organic molecule, the authors reported the stabilization of plutonium in its +IV oxidation state in the presence of each of the three ligands.

Subtask 3: Relative Impacts of Carbonate and Borate

Actinide–borate complexation has recently become a focus of research attention following the pioneering study of Borkowski et al. [Borkowski 2010]. Borax ($Na_2B_4O_7{\cdot}10H_2O$), a natural inclusion in Salado Formation salt can be present in a salt-based repository as a component of intruding brines, relict borate phases in rock salt or as part of the emplaced waste. The borate predominance concentration in the intergranular brines at WIPP is 166 ppm calculated as mono boric acid, and ranks only behind chloride and sulfate [SOTERM, 2019]. The speciation of borate in aqueous systems is highly complicated and potentially affected by pH, ionic strength and total boron concentration. The more information is required for comprehensive thermodynamic description of An-borate complexation.

Only a very limited number of experimental studies of borate complexation of selected lanthanides and actinides have been reported previously. Most of these studies focus on Nd(III), Eu(III) and Cm(III) as analogues of the trivalent actinides of Am(III) and Pu(III) [Shott 2014, Shott 2015, Hinz 2015], but a systematic study of actinide–borate complexation has not been performed.

Hinz et al. studied the interaction of borate ($0.004\ M \leq [B]_{tot} \leq 0.16\ M$) with a comprehensive series of solubility experiments in 0.1–5.0 M NaCl and 0.25–4.5 M $MgCl_2$ solutions at $7.2 \leq pH_m \leq 10.0$ ($pH_m = -\log[H^+]$) using X-ray Photoelectron Spectroscopy (XPS), X-ray Diffraction (XRD), Scanning electron microscopy (SEM) and energy dispersive X-ray spectroscopy (EDS), Ultraviolet-Visible-Near Infrared (UV-VIS-NIR) and synchrotron-based spectroscopic techniques such as X ray Absorption Spectroscopy (XAS). UV-VIS-NIR clearly indicates the formation of weak Np(V)–borate complexes under weakly alkaline pH conditions, with the likely participation of polyborate species in the complex formation. The formation of Np(V)–borate complexes has only a minor impact on the solubility of Np(V) under near-neutral to weakly alkaline pH conditions. On the contrary, a very significant drop in the Np(V) solubility (3 to 4 orders of magnitude) is observed in NaCl and dilute $MgCl_2$ solutions with $[B]_{tot} = 0.16\ M$ and $pH_m \leq 9$. XRD, XPS, SEM–EDS and XAS confirm the formation of previously unknown Na–Np(V)–$borate_{(cr)}$ and Mg–Np(V)–$borate_{(cr)}$ solid phases

in NaCl and dilute $MgCl_2$, respectively. Although the undersaturation solubility experiments with the Mg–Np(V)–borate$_{(cr)}$ phase exhibit a very low solubility in 4.5 M $MgCl_2$ solutions, the transformation of $NpO_2OH_{(am)}$ was kinetically hindered and was not observed (within the timeframe of this study) in such concentrated brines [Hinz 2020].

CO_2 is generated in the WIPP as the result of microbial degradation of coexisting CPR (cellulosic, plastic, and rubber materials) waste [CRA 2014]. This CO_2 will potentially dissolve in brine and react with the engineered barrier, MgO, to form an insoluble $MgCO_3$. Calcium and iron(II) are also present in the WIPP and will form insoluble carbonates [Borkowski 2009].

The studies showed carbonate free solutions, $NpO_2OH_{(s)}$ and $Np_2O_{5(s)}$, are considered stable solid phases [Kaszuba 1999, Kim 2006, Lierse 1985], whereas $MNpO_2CO_3{\cdot}xH_2O$ or $M_3NpO_2(CO_3)_2$ ($M = Na^+, K^+$) or both are the solubility-limiting solid phases based on the XRD in an equilibrium state containing carbonate. Therefore, one of the characteristics of the solubility-limiting solid phases of Np(V) is their strong reliance on the alkali carbonate concentration [Neck 1994, Novak 1997, Mahamid 1998].

The goal of the work is to obtain site-relevant experimental data on the solubility of Np(V) under WIPP-relevant brines as a function of pC_{H+} and ionic strength, in the absence/presence of carbonate, borate and WIPP-specific organics.

4. Experimental Description

4.1. Chemicals and Brines preparations

NaCl (Fisher Scientific, lot: 193467), HNO_3 (Fisher Scientific, lot: 1218010), NaOH (Fisher Scientific, lot: 000381) , HCl (Fisher Scientific, lot: 4108010), EDTA (Na_4EDTA, Aldrich, lot: MKBS6945V), Citrate (Citric acid anhydrous, Fluka lot: 447332/1 21403229), Acetate (Sodium Acetate, Aldrich lot: 01103TZ), Oxalate (Oxalic Acid, lot: 05829CH) $NaHCO_3$ (Fisher Scientific, lot: 041522) used in this study. All solutions were prepared with ultrapure water purified with a Milli-Q-academic (Millipore) apparatus. All solutions and samples were prepared by first degassing of high purity water with nitrogen for 5-6 hours and then handled inside an inert gas (nitrogen) glovebox at 24 ± 2 °C.

The predicted range in brine composition expected in the WIPP is shown in Table 2. In the WIPP, high ionic strength brines will form when the intruded brine reacts with the emplaced materials. These brines are Na/Mg/Cl dominated with lesser amount of calcium, borate, sulfate, potassium, lithium, bromide, and carbonate. In long term experiments, 90% strength compositions are used to prevent salt precipitation, and minimize mineral colloid, and pseudo-colloid formation. This dilution is a necessary step for anoxic experiments. More detailed

information about brine preparation and concentration of brine components can be found in [ACP-EXP-001].

Table 2. WIPP-relevant Brine Compositions of the Brines used in the Experiments.

Brine	Element/Species in M								
	Na^+	K+	Mg^{2+}	Ca^{2+}	Li^+	B_4O_72-	Cl^-	SO_4^{2-}	Br-
GWB	3.01E+00	4.14E-01	9.01E-01	1.22E-02	3.86E-03	3.49E-02	4.86E+00	1.54E-01	2.36E-02
GWB Borate free	3.10E+00	4.11E-01	9.05E-01	1.18E-02	3.87E-03	-	4.96E+00	1.53E-01	2.36E-02
pC_{H+} 9	3.45E+00	4.50E-01	1.13E+00	1.35E-02	3.70E-03	3.89E-03	5.43E+00	1.70E-01	2.35E-02
pC_{H+} 9 borate free	3.42E+00	4.62E-01	1.03E+00	1.35E-02	3.72E-03	3.89E-03	5.43E+00	1.72E-01	2.35E-02
pC_{H+} 11	4.90E+00	4.49E-01	1.10E-02	1.09E-02	3.50E-03	3.05E-02	5.31E+00	1.65E-01	2.30E-02
pC_{H+} 11 borate free	4.88E+00	4.48E-01	1.01E-02	1.09E-02	3.50E-03	-	5.30E+00	1.63E-01	2.30E-02
5 M NaCl	4.90E+00	-	-	-	-	-	4.90E+00	-	-

4.2. pH Measurements

The hydrogen ion concentration (pC_{H+}= –log [H+], in molal units) was determined according to $pC_{H+} = pH_{exp} + \Delta pH$ as described previously in the literature [Altmaier 2003 and LCO-ACP-08] where pH_{exp} is the measured pH value and ΔpH is the empirical correction factor entailing the liquid junction potential of the electrode and the activity coefficient of H^+. ΔpH values used in the present study were 0.86 for 5.0 M NaCl, 0.87 for pC_{H+} 11 and 1.12 for pC_{H+} 9 respectively.

4.3.Liquid Phase Characterization by UV-VIS-NIR

Spectrophotometric measurements were performed using a Cary 5000 (Varian) UV–VIS–NIR spectrometer in double beam mode. Measurements were conducted in the wavelength range between 300 and 1200 nm and in gas-tight cuvettes. Spectra were recorded with a 0.2 nm data

interval, a scan rate of 60 nm.min^{-1} and a band pass of 0.6 nm. Sampling for UV VIS analysis was performed after 60 days.

Selected samples with sufficient Np concentration, approximately [Np] $\geq 3 \times 10^{-6}$ M, were centrifuged through a 10 kDa filter (Pall-type filters, Omega-modified polyethersulfone) with 13000 RPM centrifugation during 30 minutes prior to UV-VIS-NIR measurements in a glovebox to separate suspended solid phase particles. Separate baselines are recorded for each pC_{H+}, ionic strength condition and ligand concentration. Three absorption spectra were collected sequentially for each sample at 25 °C and merged into one spectrum as shown.

4.4. Np Stock Solution Preparation

^{237}Np obtained from Oak Ridge National Laboratory with ^{237}Np % 99.99 and ^{236}Np < % 0.01, ^{235}Np < 0.001 purity in oxide form (NpO_2) with black powder (Batch ^{237}Np-4157). 75 mg NpO_2 was weighed and put in 5 mL concentrated HNO_3 to dissolve. The Np solution in concentrated HNO_3 was then heated about 130 °C in a glass vial on a hot plate to dryness. During evaporation time, black powder was dissolved, and a dark green Np solution was observed. This indicated changing oxidation state from IV to V and VI oxidation state of Np. 5 mL of 1 M HCl was added to the dried Np solution and evaporated again to remove NO_3^- from the solution. This was repeated three times. 4 mL 1 M $NaHCO_3$ at pH 9 was added immediately. Finally, the pH value of the solution was between 8 and 9. White $NaNpO_2CO_3$ precipitation was observed. Subsequently, the $NaNpO_2CO_3$ precipitate was separated by decanting. 1-2 ml white $NaNpO_2CO_3$ suspension was dissolved with 5 mL 1 M HCl.

The pH of Np stock solution was checked again to be sure that solution does not contain any carbonate. A pH value of < 1 indicates that the solution does not contain carbonate. At the end, greenish color solution was observed. The Np Stock solution was analyzed by UV-VIS-NIR to determine oxidation state. UV-VIS-NIR spectrum showed a main peak of Np(V) ions at 981 nm and indicated the solution has 100 % Np(V) [Petrov 2016]. This Np(V) stock solution was used for solubility experiments and to prepare Np(IV) and Np(V) standards (XANES reference spectrum) to use Linear Combination Fit Analysis (LCFA) of XANES spectrum.

A aliquot of Np(V) stock solution in 1 M HCl was separated to generate Np(IV) stock solution. First, the solution was evaporated by heating, then 0.1 M HCl was added to the dried Np. A small amount of this was then added to concentrate HBr. The final solution was checked by UV VIS NIR spectrometer. Absorption peak at 970 nm indicated that solution contained 100% Np(IV).

4.5.Solid Phase Preparation and Solubility Experiments

Aliquots of the Np stock solution were precipitated with carbonate free 1 M NaOH at pH ~10.5. The resulting greenish $NpO_2OH_{(am)}$ solid was washed twice with high purity water at pH 10.5. The greenish solid phase containing tube was shaken for homogenization between solid and liquid phase and 50 µL was taken and put in 10 kDa Pall nanossep Centrifugal Devices with Omega™ Membrane. This dried $NpO_2OH_{(am)}$ phase over filter cake was analyzed using XRD and SEM for determination of NpO_2OH in amorphous phase. The inventory of ^{237}Np in each sample was ~0.5 mg. Samples were equilibrated in following background electrolyte according to under saturated approach.

- in 5 M NaCl at pC_{H+} 7, 9 and 11
- in 90 % GWB at pC_{H+} 7
- pC_{H+} transitional brine at 9
- pC_{H+} transitional brine at 11

Samples systematically monitored up to 150 days for pH and concentration of Np. The aqueous concentration of Np was measured after 10 kD (~2–3 nm) ultrafiltration by ICP-MS in 14 days, 50 days and 150 days. 10 µL from each filtrate was added to 1790µL of 2% HNO_3 (Fisher Scientific, Lot: 1218110 with 300 ppb of an indium internal standard (Agilent high purity metal standard, lot: 2013216) to provide a final dilution of 1:180 in duplicate for (Inductively Coupled Plasma-Mass-Spectrometry) ICP-MS analysis. More detailed information about ICP-MS measurements can be found in [ACP-EXP-011].

4.6. XANES Data Evaluation

XAS experiments were performed at 10-BM beamline at the Advanced Photon Source (APS), Argonne National Laboratory (ANL) [Kropf 2010]. The flux of X-rays before and after transmitting through the sample were measured in ion chambers containing suitable gases in suitable proportion which are 75 % Argon, 8 % Nitrogen and 17% Helium .

Bulk XAS data at the Np L_{III}-edge at 17610 eV were collected in fluorescence mode at room temperature using a four element Ge solid-state detector. The beamline is equipped with a Ge(422) double crystal water chilled Si(311) double crystal monochromator. The energy calibration was carried out after each sample by the measurement of a Zr foil (Zr K-edge at 17998 eV). The XAS data analysis was performed with the ATHENA software program [Ravel 2005]. The average oxidation state of Np in the bulk EXAFS samples was determined by fitting the XANES region between 17605 and 17725 eV by a linear combination fit of standard spectra Np(IV) and Np(V).

5. Results and Discussion

5.1.UV-VIS-NIR Results

UV-VIS-NIR spectroscopy has been widely used to study the complexation reactions of $Np(V)O_2^+$ in high ionic strength alkali brine solutions. The technique has a sensitivity to $Np(V)O_2^+$ species, which can be characterized because the $Np(V)O_2^+$ exhibits Laporte forbidden f-f transitions. Complexation reactions of the non-complexed ion can be tracked because the absorption band (λ_{max}) is shifted significantly with the addition of ligands.

5.1.1. Np in 5 M NaCl Investigation by UV-VIS-NIR

In order to verify the species of Np and determine the amount of Np oxidation state after 60 days in 5 M NaCl in function of pC_{H+} at 7, 9, 11, aqueous phases in equilibrium with $Np(V)O_2OH_{(am)}$ solids were investigated for selected samples with a sufficient Np concentration level. Investigation was done by UV-VIS-NIR absorption spectroscopy. The NIR spectra of Np in the wavelength region between 950 and 1040 nm are displayed in Figure 1 for the untreated alkaline samples in 5.0 M NaCl (pC_{H+} =7, 9, 11) and the corresponding supernatant after addition of 10 µL 1 M HCl (resulting $pC_{H+} \sim 2$) in the cuvette, and second measurement recorded to acidified samples. The black line on Figure 1 represents the spectrum of the $Np(V)O_2^+$ stock solution of about 1.10^{-5} M in 1 M HCl. The NIR band of the $Np(V)O_2^+$ aquo ion is located at 981 ± 0.2 nm with a molar absorption coefficient of $\varepsilon = 395\ M^{-1}\cdot cm^{-1}$.

In the NIR spectra of the nonacidified alkaline sample supernatant, the absorption intensity of Np(V) at λ = 981–982 nm systematically decreases with increasing pC_{H+} value depending on the solubility properties of Np in different pC_{H+}. A shoulder appears at higher wavelength (about 985 nm), which indicates contributions from another Np(V) species. The slight a shift peak shift indicated contributions from Np(V) chloro complexes, $NpO_2(OH_2)_{5-n}Cl_n^{1-n}$ and Np(V) hydrolysis species, $NpO_2(OH_2)_{5-m}(OH)^{1-m}$. Similar results for Np(V) in NaCl, $CaCl_2$ solutions were reported in [Petrov 2017, Neck 1995a, Fellhauer 2016], respectively. The slight deviations in the spectral features observed are due to contributions from Np(V) chloro complex to all spectra of acidified samples at pC_{H+} : 7, 9, 11 in 5 M NaCl. This is very similar to what was reported for the Np(V) in 5 M NaCl after acidification with its characteristic absorbance at λ_{max} =981 nm [Petrov 2017].

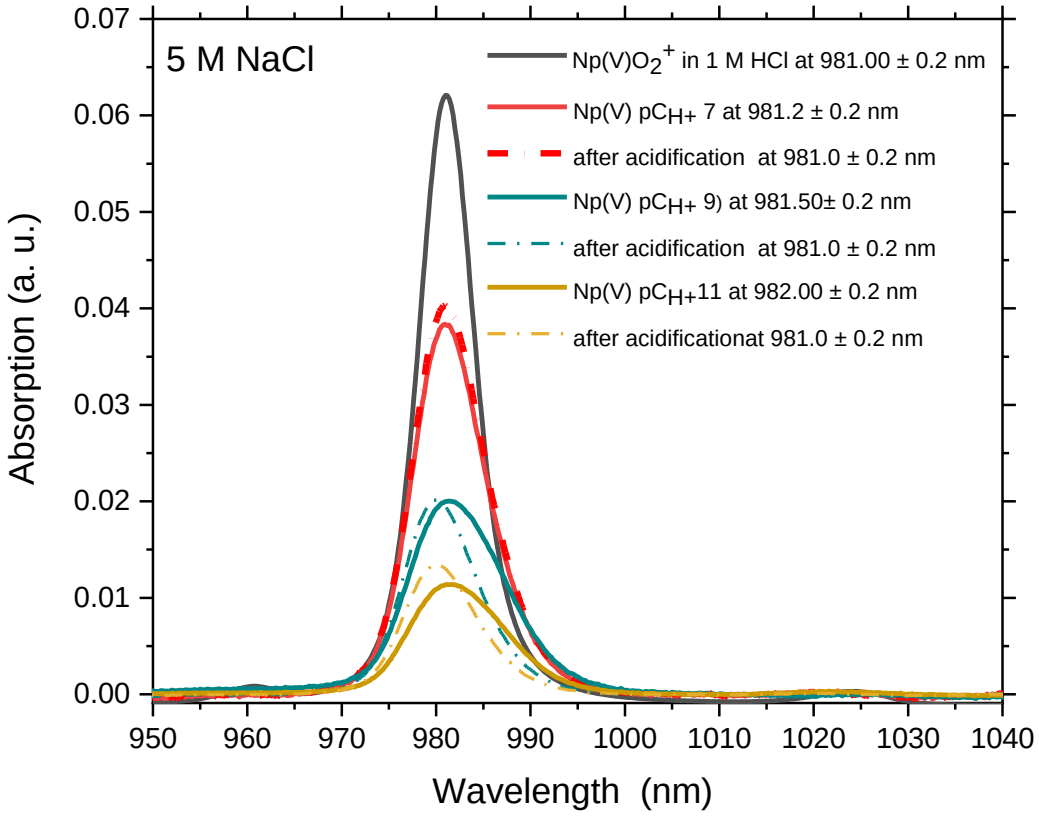

Figure 1. NIR absorption spectra of supernatant solutions in equilibrium with $NpO_2OH_{(am, fresh)}$ in 5.0 M NaCl at pC_{H+} 7 , 9 , 11. Dash Spectrum represent acidified sample in the cuvette with 1 M HCl after the measurement, and a second spectrum was recorded to compare Np(V) stock solution in 1 M HCl.

UV-VIS-NIR confirms the only oxidation state of Np(V) in the aqua phase after 60 days. The results of the present methods lead to the conclusion that the interaction between $Np(V)O_2^+$ and Cl^- ions is to be treated as strong ion-ion interaction.

5.1.2. Np in WIPP brine investigation by UV-VIS-NIR

Samples from ongoing Np solubility experiments on the 60th day in synthetic WIPP brine at pC_{H+} 7 and 11 were analyzed by UV-VIS-NIR spectroscopy. Spectra are shown in Figure 2. A red shift of the absorption band is observed for both samples from different pC_{H+}, which are Np(V) at pC_{H+} 7 with max absorption at 984 nm and Np(V) in pC_{H+} 9 brines with max absorption at 986.4 nm. This indicates that different NpO_2^+ complexes are formed in synthetic WIPP brine.

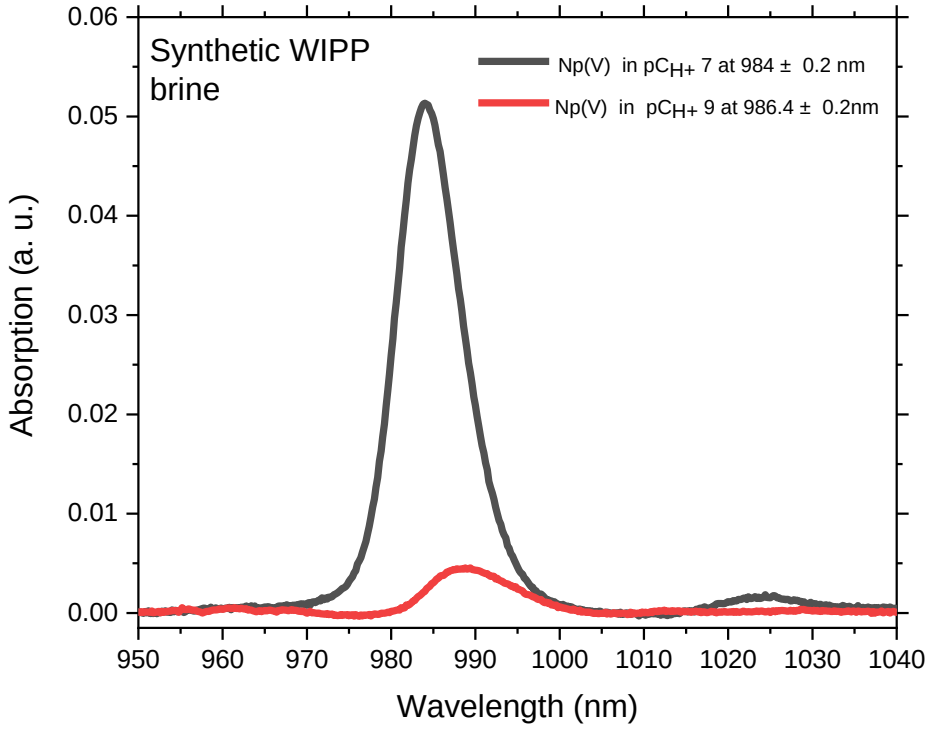

Figure 2. NIR absorption spectra of supernatant solutions in equilibrium with $NpO_2OH_{(am, fresh)}$ in synthetic WIPP brine at pC_{H+} 7 and 9.

Max. absorption shifts in synthetic brine samples are more noticeable than Np(V) in 5 M NaCl which was discussed in the previous section. The main reason for this is that synthetic WIPP brine contains more than one component that can form multiple Np species such as $NpO_2Cl(aq)$.

Maiwald et al. has studied Np(V)-Sulfate interaction in aqueous solution in function of total ligand concentration (Na_2SO_4), ionic strength ($NaClO_4$), and temperature (T = 20–85 ^oC) at pH 4.3 by using UV-VIS-NIR. He proved a single complex species $NpO_2(SO_4)^-$ at 983.1 nm was identified by peak deconvolution of the absorption spectra [Maiwald 2018].

As a result, however, literature information and the absorption band shift observed in this study confirm that Np can simultaneously form a complex with one or more components in the UV-VIS-NIR. It is very difficult to say anything about the ratios of the new species, which are formed by these components with Np. Nevertheless, UV-VIS-NIR confirms the predominant oxidation state of Np(V) in the aqua phase of WIPP brine at pC_{H+}7 and 9 after 60 days.

5.1.3. Np-Borate Interaction in WIPP Brine and 5 M NaCl

In order to understand the borate effect on Np speciation in WIPP brine system, two additional samples in pC_{H+} 7 and pC_{H+} 9 in synthetic WIPP brine without borate were measured by UV-VIS-NIR. In addition, the interaction of Np(V) with 10 mM ≤ $[B]_{tot}$ ≥ 160 mM in 5 M NaCl at pC_{H+} 7 and in pC_{H+} 9 was investigated systemically. All results are shown in Figure 3.
Np(V) absorption spectra of synthetic WIPP brine pC_{H+} 7 and pC_{H+} 9 in the absence of borate show the characteristic NpO_2^+ absorption band with a peak maximum of λ_{max} ~ 981.7 nm at pC_{H+} 7 and λ_{max} ~ 981.9 nm at pC_{H+} 9. This weak peak shift to higher wavelength can be caused by the presence of chloro, sulfate or other brine components forming new Np-Species.

At very low $[B]_{tot}$ = 10 mM in the 5 M NaCl at pC_{H+} 7 and 9 system, weak peak shift to higher wavelengths can be observed, indicating that un-complexed NpO_2^+ predominates in 5 M NaCl.
In both systems (pC_{H+}7 and 9 in 5 M NaCl), for increasing with $[B]_{tot}$ the intensities of the absorption band decrease and peak maxima are shifted to higher wavelengths. The results clearly indicate the formation of a Np(V)–borate complex in 5 M NaCl at pC_{H+}7 and pC_{H+}:9. The more pronounced shift and broadening of the peak observed at pC_{H+} 9 indicate stronger influence of borate on the Np(V) speciation at higher pC_{H+}, and the possible formation of more than one Np(V) borate species.

The speciation of borate is highly complex. Several borate species, whose concentration is strongly dependent on pC_{H+}, $[B]_{tot}$, type and concentration of background electrolyte, could behave as possible complexing ligands.

Hinz at al. also studied the interaction of Np with borate in 0.1–5.0 M NaCl and 0.25–4.5 M $MgCl_2$ solutions with 7.2 ≤ pC_{H+} ≤ 10.0 and 0.004 M ≤ $[B]_{tot}$ ≤ 0.16 M using UV-VIS-NIR and other spectroscopic methods. A red shift (≈5 nm) in the Np(V) band at λ = 980 nm indicates the formation of weak Np(V)–borate complexes under mildly alkaline pH_m-conditions. The identification of an isosbestic point supports the formation of a single Np(V)–borate species in dilute $MgCl_2$ systems, whereas a more complex aqueous speciation (eventually involving the formation of several Np(V)–borate species) is observed in concentrated $MgCl_2$ solutions [Hinz 2020].

Solubility studies with $NpO_2OH_{(am)}$ combined with UV-Vis-NIR investigations confirm that the presence of borate strongly affects the aqueous speciation of Np(V) in solutions at pC_{H+}7 and 9. UV-VIS-NIR confirms the predominant oxidation state of Np(V)in the aqua phase after 60 days.

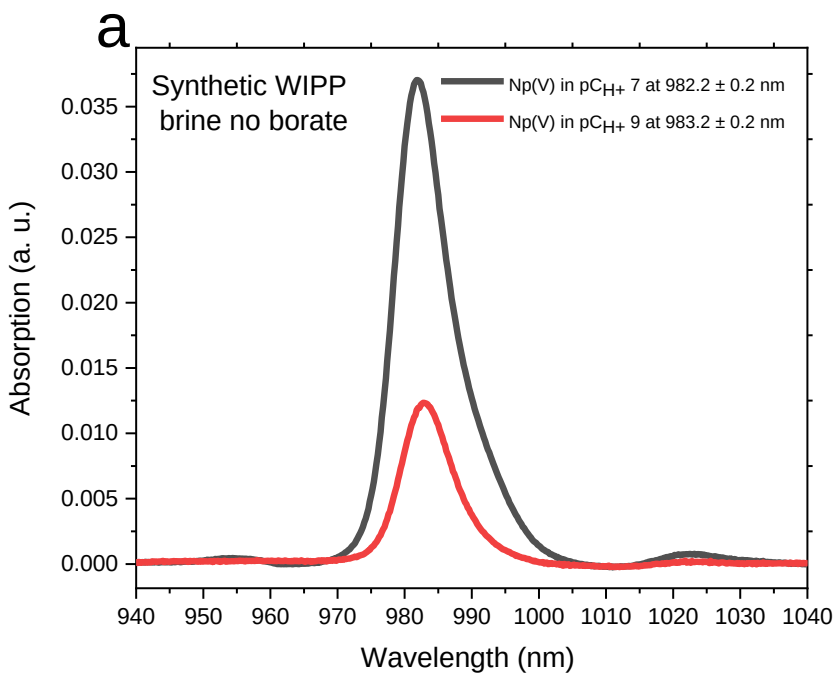
a
Synthetic WIPP
brine no borate
Np(V) in pC$_{H+}$ 7 at 982.2 ± 0.2 nm
Np(V) in pC$_{H+}$ 9 at 983.2 ± 0.2 nm
Absorption (a. u.)
0.035
0.030
0.025
0.020
0.015
0.010
0.005
0.000
940 950 960 970 980 990 1000 1010 1020 1030 1040
Wavelength (nm)

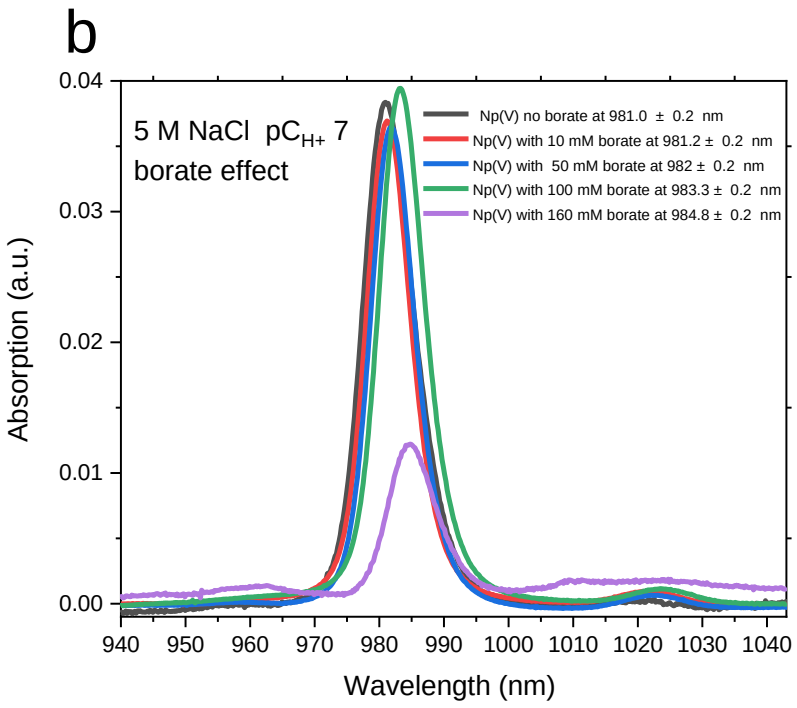
b
5 M NaCl pC$_{H+}$ 7
borate effect
Np(V) no borate at 981.0 ± 0.2 nm
Np(V) with 10 mM borate at 981.2 ± 0.2 nm
Np(V) with 50 mM borate at 982 ± 0.2 nm
Np(V) with 100 mM borate at 983.3 ± 0.2 nm
Np(V) with 160 mM borate at 984.8 ± 0.2 nm
Absorption (a.u.)
0.04
0.03
0.02
0.01
0.00
940 950 960 970 980 990 1000 1010 1020 1030 1040
Wavelength (nm)

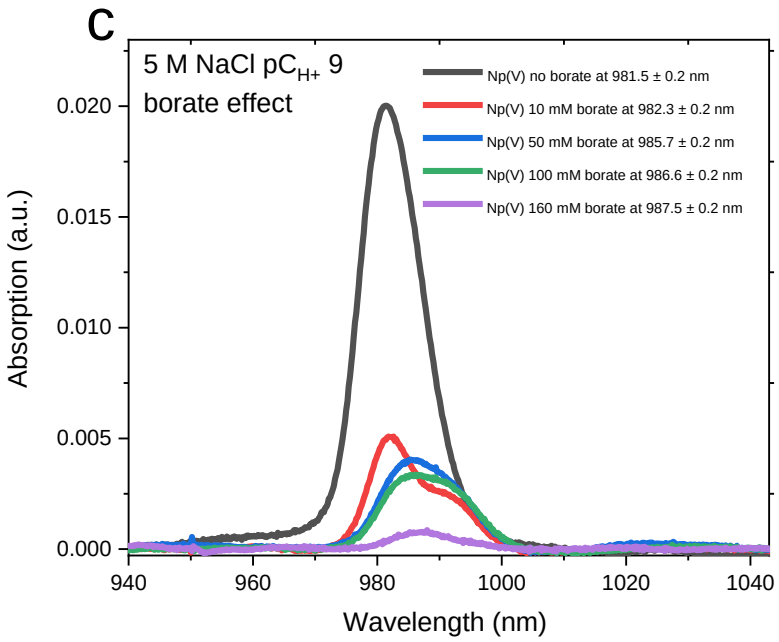

Figure 3. NIR absorption spectra of supernatant solutions in equilibrium with $NpO_2OH_{(am, fresh)}$ a) in synthetic WIPP brine absence of borate at pC_{H+}7 and pC_{H+} 9 b) in 5.0 M NaCl at pC_{H+} 7 in function of borate concentration c) in 5.0 M NaCl at pC_{H+} 9 in function of borate concentration.

5.2. XANES Results

Figure 4 shows the Np-L_{III} XANES spectra of the solid phases from under saturated experiments. For comparison purpose Figure 4 also show the $Np(IV)(OH)_4(s)$ and $Np(V)O_2OH(s)$ standard spectrum. In contrast to Np(IV), Np(V) is known to form trans dioxo cations. This is the reason why the Np-$L_{(III)}$-edge XANES spectra of Np(V) differs from that of Np(IV). As can be seen from Figure 4, and Table 3 the increase in the formal oxidation state from IV to V leads to a small shift of the absorption edge by approximately 1 eV toward higher energy. The observed spectral features allow to distinguish between these two different Np oxidation states by Np-L_{III}-edge XANES spectroscopy. The oxidation state of Np-L_{III}-edge XANES based on the shape and energy position of the white line agrees with solid Np(V) reference samples in Figure 4 and Table 3.
The oxidation state of Np in the samples was determined by fitting the XANES region between 17605 and 17725 eV by a linear combination of reference spectra Np(IV) and Np(V). A more detailed analysis employing linear combination fitting analysis (LCFA) based on reference spectra show that all measured sample consist of 100 % Np(V) with ± 8 % error. Experimental data and corresponding fit from LCFA are shown in Figure 4.

Table 3. Energy positions of the Np L_{III}-edge XANES first inflection point and white line maximum for aqueous and solid Np(V) references and the seven samples investigated in the present work and two reference spectrum (Np(IV) and Np(V)). All values are given in eV (estimated calibration error ΔE ± 0.2 eV).

Sample	**First inflection point (eV)**	**White line maximum (eV)**
Np(V)ref. aq [Brendebach 2005]	17 609.0	17 614.0
Np(V)ref. solid [Goana 2012]	17 607.7	17 612.7
Np(V) ref. $Np(V)O_2OH(am)$	17609.8	17617.8
Np(IV) ref. $Np(IV)(OH)_4(am)$	17610.6	17618.2
NpO2(OH)(am) starting material	17609.4	17615.5
Np(V) WIPP in 5 M NaCl at pC_{H+} 9	17609.0	17616.3
Np(V) synthetic WIPP brine at pC_{H+} 9	17609.4	17617.1
Np(V) synthetic WIPP brine at pC_{H+} 9 –borate free	17608.6	17616.1
Np(V) 5 M NaCl at pC_{H+} 9 – 160 mM borate	17608.6	17616.0
Np(V) in synthetic WIPP brine at pC_{H+} 9 – 160 mM carbonate	17609.2	17616.5
Np(V) 5 M NaCl at pC_{H+} 9 – 100 mM carbonate	17609.6	17616.6

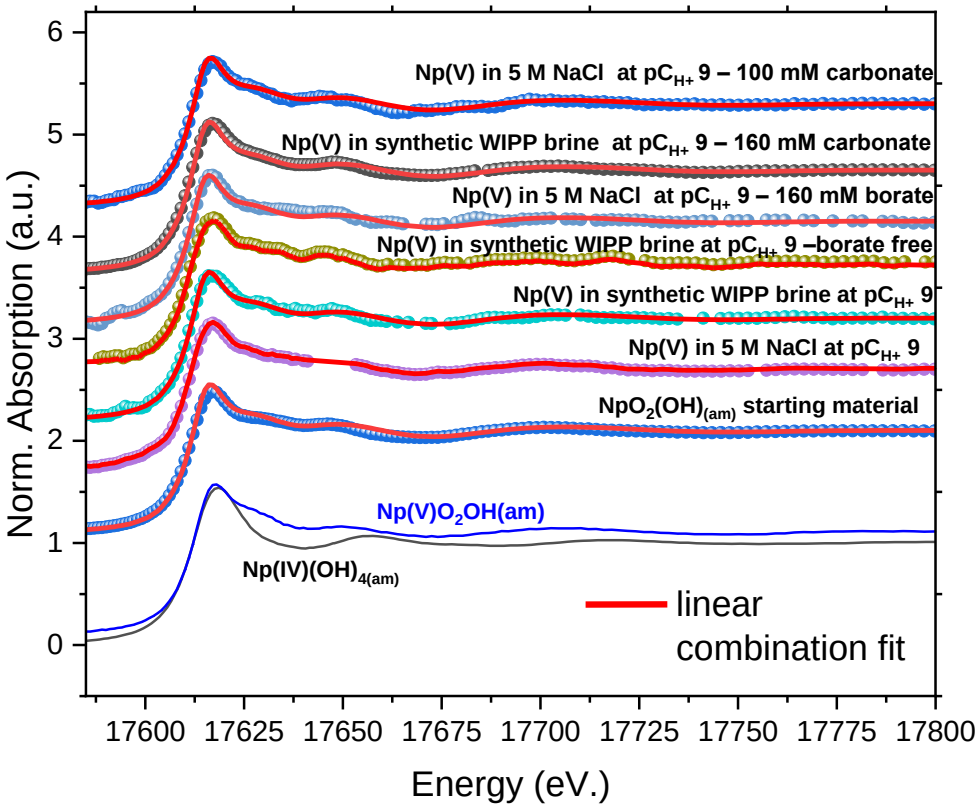

Figure 4. Experimental Np-L_{III}-edge XANES spectra. Each experimental data are compared to corresponding linear combination fits of Np(IV) and Np(V).

5.3. Solubility Results

5.3.1. Subtask 1: Apparent Solubility of Np(V) under WIPP-relevant Conditions

The effect of WIPP relevant ligands on Np(V) solubility in synthetic WIPP brine at pC_{H+} 7, 9 and 11 was summarized in Figure 5. The Np(V) concentrations slightly decrease in synthetic WIPP brine dependent of the presence of WIPP organic and all organic ligands inclusive carbonate show same effect on Np(V) solubility at pC_{H+} 7. From first sampling (14 days), it is seen that Np has reached equilibrium, the Np concentration has barely changed in 150 days presence of ligands in synthetic WIPP brine at pC_{H+} 7 (for time depending results can be found in Figure 9 in Appendix). Carbonate also had an impact on the observed Np solubility in WIPP brine at pC_{H+} 9. The experiments with the carbonate content of 16.10^{-3} M, the Np concentrations reached about 4.10^{-7} M, which was more than one orders of magnitude lower than in the absence of carbonate. This important result indicate for the accuracy of the WIPP conceptional model. The thermodynamic

database for the An(V) actinides currently used in EQ3/6 is described by [Giambalvo 2002]. Np(V) speciation and solubility were parameterized in the Pitzer activity-coefficient model for the Na^+- K^+ - Mg^{2+} - Cl^-- SO_4^{2-}- CO_3^{2-}- HCO_3^- - OH^-- H_2O system. The model contains the solid species $NpO_2OH_{(am)}$, $NpO_2OH_{(aged)}$, $Na_3NpO2(CO_3)_{2(s)}$, $KNpO_2CO_3{\cdot}2H_2O_{(s)}$, $K_3NpO_2(CO_3)2{\cdot}0.5H_2O_{(s)}$, and $NaNpO_2CO_3{\cdot}3.5H_2O_{(s)}$ to explain the available data. Aqueous and solubility-limiting species [CRA 2019] for Np(V) that are used for the An(V) WIPP model are given in Table 4, 5 and 6.

Table 4. Solid formation reactions of Np(V) in WIPP relevant conditions [SOTERM, 2019]

Np(V) Solid formation Reactions	**log K**	
$NpO^{2+} + OH^- \leftrightarrows NpO_2OH_{(s,\ aged)}$	9.5	(SOTERM.56)
$NpO^{2+} + OH^- \leftrightarrows NpO_2OH_{(s,\ am)}$	8.8	(SOTERM.57)
$Na^+ + NpO_2^+ + CO_3^{2-} + 3.5H_2O \leftrightarrows NaNpO_2(CO_3){\cdot}3.5H_2O_{(s)}$	11.1	(SOTERM.58)
$3Na^+ + NpO_2^+ + 2CO_3^{2-} \leftrightarrows Na_3NpO_2(CO_3)_{2(s)}$	14.2	(SOTERM.59)
$K^+ + NpO^{2+} + CO_3^{2-} \leftrightarrows KNpO_2(CO_3)_{(s)}$	13.6	(SOTERM.60)
$3K^+ + NpO_2^+ + 2CO_3^{2-} + 0.5H_2O \leftrightarrows K_3NpO_2(CO_3)_2{\cdot}0.5H_2O(s)$	-4.8	(SOTERM.61)

Table 5. Inorganic aqueous formation of Np(V) in WIPP relevant conditions

Np(V) Inorganic Aqueous Formation Reactions	Log K	
$NpO_2^+ + OH^- \leftrightarrows NpO_2OH_{(aq)}$	2.7	(SOTERM.62)
$NpO_2^+ + 2OH^- \leftrightarrows NpO_2(OH)^{2-}$	4.5	(SOTERM.63)
$NpO_2^+ + CO_3^{2-} \leftrightarrows NpO_2CO_3^-$	5.0	(SOTERM.64)
$NpO_2^+ + 2CO_3^{2-} \leftrightarrows NpO_2(CO_3)_2^{3-}$	6.4	(SOTERM.65)
$NpO_2^+ + 3CO_3^{2-} \leftrightarrows NpO_2(CO_3)_3^{5-}$	5.3	(SOTERM.66)

Table 6. Organic aqueous formation of Np(V) in WIPP relevant conditions

Np(V) Organic Aqueous Formation Reaction	Log K	
$NpO_2^+ + Acetate^- \leftrightarrows NpO_2Acetate(aq)$	1.37	(SOTERM.67)
$NpO_2^+ + Citrate^{3-} \leftrightarrows NpO_2Citrate^{2-}$	3.50	(SOTERM.68)
$NpO_2^+ + EDTA^{4-} + 2H_2O \leftrightarrows NpO_2H_2EDTA^- + 2OH^-$	-7.1	(SOTERM.69)
$NpO_2^+ + EDTA^{4-} + H_2O \leftrightarrows NpO_2HEDTA^{2-} + OH^-$	1.5	(SOTERM.70)
$NpO_2^+ + EDTA^{4-} \leftrightarrows NpO_2EDTA^{3-}$	8.54	(SOTERM.71)
$NpO_2^+ + Oxalate^{2-} \leftrightarrows NpO_2Oxalate^-$	4.24	(SOTERM.73)

All WIPP relevant organic ligands with carbonate and without carbonate show same Np solubility behavior at pC_{H+} 9. The presence of these ligands in WIPP brine at pC_{H+} 9 decreases the concentration of Np(V) by approximately one orders of magnitude (see figure 5).

Lastly, the third pC_{H+} of interest is at pC_{H+}11. In that pC_{H+}, the Np(V) concentrations were stable around 10^{-7} M. Presence of carbonate with other organic ligands and single carbonate ligand in the WIPP brine increase Np(V) solubility at pC_{H+} 11. Also there is no effect observed, presence of and absence of organic on Np solubility at pC_{H+} 11.

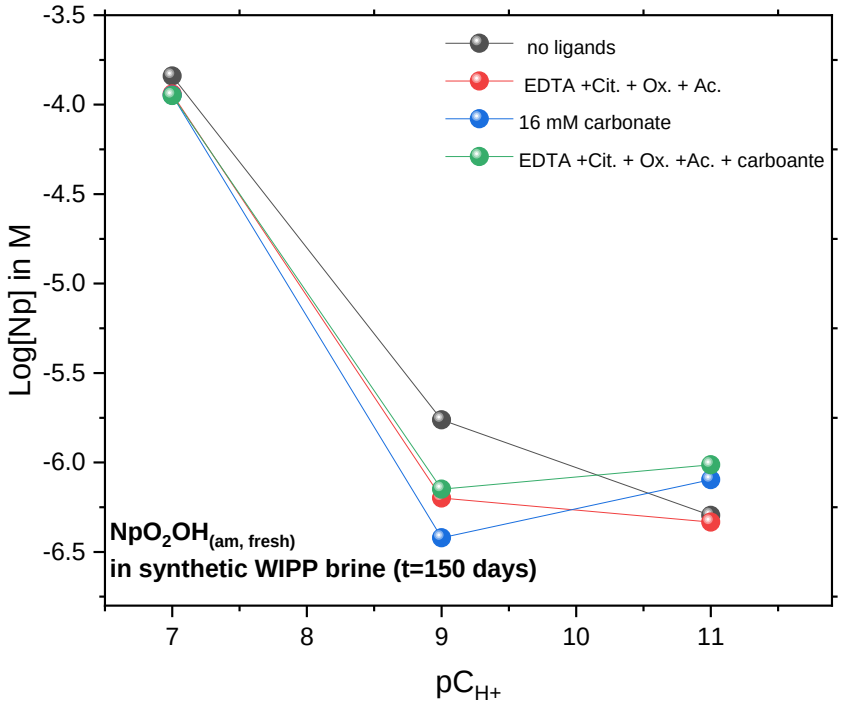

Figure 5. Solubility of $NpO_2(OH)_{(am,\ fresh)}$ in the absence and presence of (in)organic ligands Citrate: 2.30 x 10^{-3} M, Acetate: 2.83 x 10^{-2} M, Oxalate: 1.13 x 10^{-2} M, EDTA: 7.92 x 10-5 M, and Carbonate: 1.6 x 10^{-2} M) in synthetic WIPP brine solutions as a function of pC_{H+}.

5.3.2. Subtask 2: Screening Experiments with Organic Complexants to Confirm Model Predictions

Figure 6 shows the solubility of $NpO_2(OH)_{(am)}$ in the absence and presence of organic ligands; Citrate, Acetate, Oxalate, EDTA as a function of time in the under saturation experiments in synthetic WIPP brine at pC_{H+} 9. Over approximately 150 days, there is notable change of the solubility of Np(V) in the presence of organic ligands. It is seen that $NpO_2(Ac)_{(aq)}$ species in synthetic WIPP brine at pC_{H+} 9 is dominant species from the first sampling (t=14 d to the last sampling date 150 d). Domski and Sisk-Scott calculated Np soluble speciation presence of organic

ligands in GWB by using solubility-controlling solid was $KNpO_2CO_3$. Our results overlap with the results of the Np in WIPP brine thermodynamic calculation [Domski and Sisk-Scott 2019]. The interactions of EDTA, Citrate, Acetate and Oxalate with Np(V) vary depending on kinetics. In the first sampling, EDTA and Citrate presence increase the solubility of Np(V) by half order of magnitude than absence of organic in the sample. However second and third sampling results shows that EDTA and Citrate don't effect of Np(V) solubility in described conditions. The Np(V) solubility in the WIPP brine at pC_{H+} 9, all organics are present at the same time, shows a different solubility tendency than other samples. In the third sampling at the end of 150 days, Np(V) solubility in which all organics present was approximately half a log lower. However, effect of oxalate on Np(V) solubility depend on the kinetic. In the first sampling shows the lowest solubility of Np(V) n the presence of oxalate, but by the time, in the third sampling, oxalate doesn't show any significant solubility effect on Np(V) solubility. Considering the reaction kinetics, it has not been observed that the Np concentration has reached an equilibrium as a result of third samplings (for time depending results can be found in Figure 9 in Appendix).

Complexation reactions and corresponding stability for Np(V) species expected under WIPP conditions is listed in Table 7. According to these results, the most important reactions for Np(V) speciation at $pC_{H+} \cong 9$ are acetate complexation. Therefore, Np(V) complexes with organic ligands are important to the WIPP chemistry model and do make a significant contribution to the total solubility of Np(V).

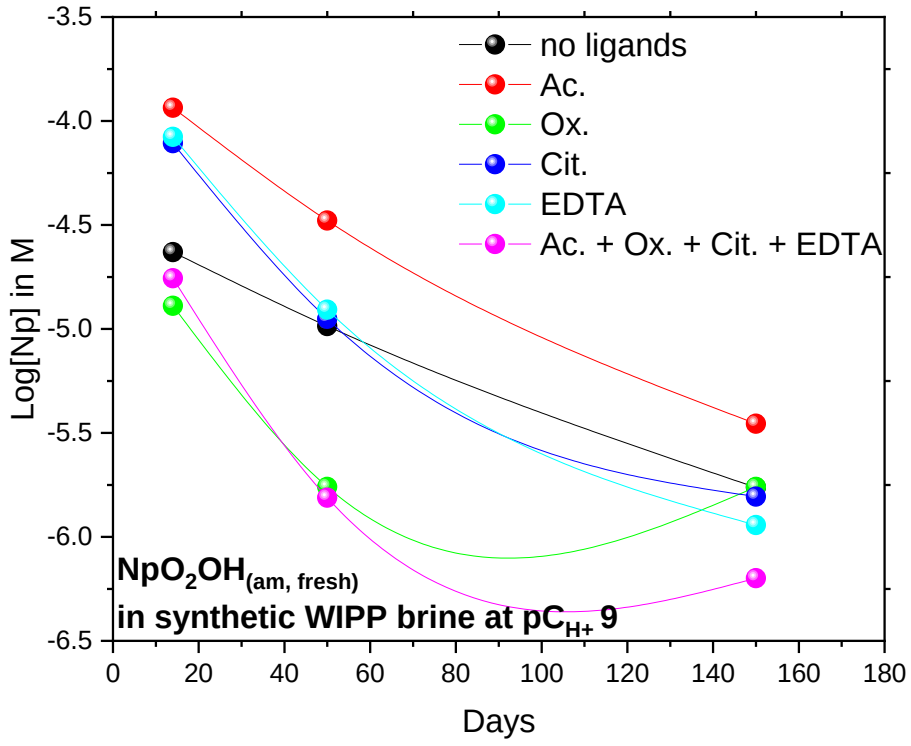

Figure 6. Solubility of $NpO_2(OH)_{(am, fresh)}$ in the absence and presence of organic ligands "Citrate: 2.30 x 10^{-3} M, Acetate: 2.83 x 10^{-2} M, Oxalate: 1.13 x 10^{-2} M, EDTA: 7.92 x 10^{-5} M", as a function of time in in synthetic WIPP brine solution.

Table 7. Predominant Speciation for the An(V) Actinides in the WIPP Species [Domski and Sisk-Scott 2019]

	% Contribution to GWB	**% Contribution to ERDA-6**
$NpO_2(Ac)$ (aq)	58.34	81.50
NpO_{2+} (aquo)	17.52	8.02
$NpO_2CO_3^-$	16.12	6.67
NpO_2Ox-	6.66	2.79
NpO_2Cit^{2-}	0.85	0.61
$NpO_2(OH)$ (aq)	0.35	0.34
Total % of Species Present	99.84	99.93

5.3.3. Subtask 3: Relative Impacts of Carbonate and Borate

Borate effect on Np solubility:

The effect of $[B]_{tot}$ (10mM ≤ $[B]_{tot}$ ≤ 160 mM) on Np solubility in 5 M NaCl and synthetic WIPP brines at pC_{H+} 7, 9 and 11 was summarized in Figure 7. For comparison purposes, Figure 7 also show the experimental solubility data for $NpO_2(OH)$(am, fresh) [Petrov et al 2017], $NpO_2(OH)_{(aged)}$ [Runde 1995], $NpO_2(OH)_{(am,\ fresh)}$ and $NaNpO_2$-Borate(cr) [Hinz 2020]. Effect of borate on Np solubility under WIPP repository conditions with presence and absence of $[B]_{tot}$= 160 mM in synthetic WIPP brines are presented in Figure 7 as a function of pC_{H+}.

Neither low borate concentration nor high borate concentration had a significant effect on the solubility of Np at pC_{H+} 7 in 5 M NaCl solution. A similar solubility behavior was observed in synthetic WIPP brine and borate free synthetic WIPP brine at pC_{H+} 7.

The Np solubility behavior at pC_{H+} ≈ 9 in the absence of borate is in good agreement with the solubility of $NpO_2OH_{(aged)}$ in 5 M NaCl [Runde 1995]. Np solubility at pC_{H+} ≈ 9 absence of borate is within the same order of magnitude of solubility of NpO_2OH(am) in 5 M NaCl [Petrov 2017].

At pC_{H+} values higher than 7 (pC_{H+} ≈ 9), Np-borate interaction was observed in 5 M NaCl and synthetic WIPP brines. It was significant that at pC_{H+} 9 the concentration of Np in 5 M NaCl decreased with increasing borate concentration. $[B]_{tot}$ ≥ 10 mM which suggests that Np(V)–borate complexes are being formed in solution. This observation clearly indicates the transformation of $NpO_2(OH)$(am) into a new solubility controlling Np-borate solid phase. The solubility limit of Np(V) in 5 M NaCl in the presence of $[B]_{tot}$ 160 mM is more than 2.5 orders of magnitude lower than those observed in the absence of borate at pC_{H+} 9. Hinz et al. reported similar observations for $NpO_2OH_{(am)}$ in 5 M NaCl in the presence of comparable borate concentrations and pC_{H+} [Hinz 2020].

The Np solubility behavior in the absence of borate in 5 M NaCl in alkaline conditions (pC_{H+} ≈ 9) overlaps with previous studies in the literature [Runde 1995, Petrov 2017]. Under hyper alkaline conditions at pC_{H+} 11 very scattered solubility data are obtained. pC_{H+} 9 has a similar tendency to the behavior observed at pC_{H+} 11 in 5 M NaCl solutions, the solubility of Np(V) decreased slowly and attained a constant value (≈5.10^{-7} M) for 100mM ≥ $[B]_{tot}$ after 180 days. Same borate effect on Np solubility in synthetic WIPP brine was observed at pC_{H+} 11. Presence of borate in synthetic WIPP brine decreased Np solubility in pC_{H+}11 approximately 1 order of magnitude and 0.5 log units at pC_{H+} 11.

The Np solubility results at pC_{H+} 11 show different kinetic behavior to that at pC_{H+} 7 and pC_{H+} 9. It was found that the Np concentration at pC_{H+} 7 still did not reach equilibrium when sampling after 150 days. The significant decrease of Np concentration in 5.0 M NaCl solutions at pC_{H+} 9 was already observed in second sampling (t= 50 days). It shows that the Np and borate interaction

started between first (14 days) and second (50 days) sampling. But kinetic of Np solubility at pC_{H+} 11 already reached equilibrium after the first sampling. This indicates that the newly formed Np-Borate solid phase at pC_{H+} 11 is the result of this fast reaction than pC_{H+} 9 and pC_{H+} 7. (For time depending results can be found in Figure 10 and 11 in Appendix).

Hinz et al. performed multimethod solid phase characterization using XRD, XPS, SEM–EDS, TEM and XAS to confirm the formation of hitherto unknown Na–Np(V)–Borate$_{(cr)}$ solid phases in NaCl [Hinz 2020].

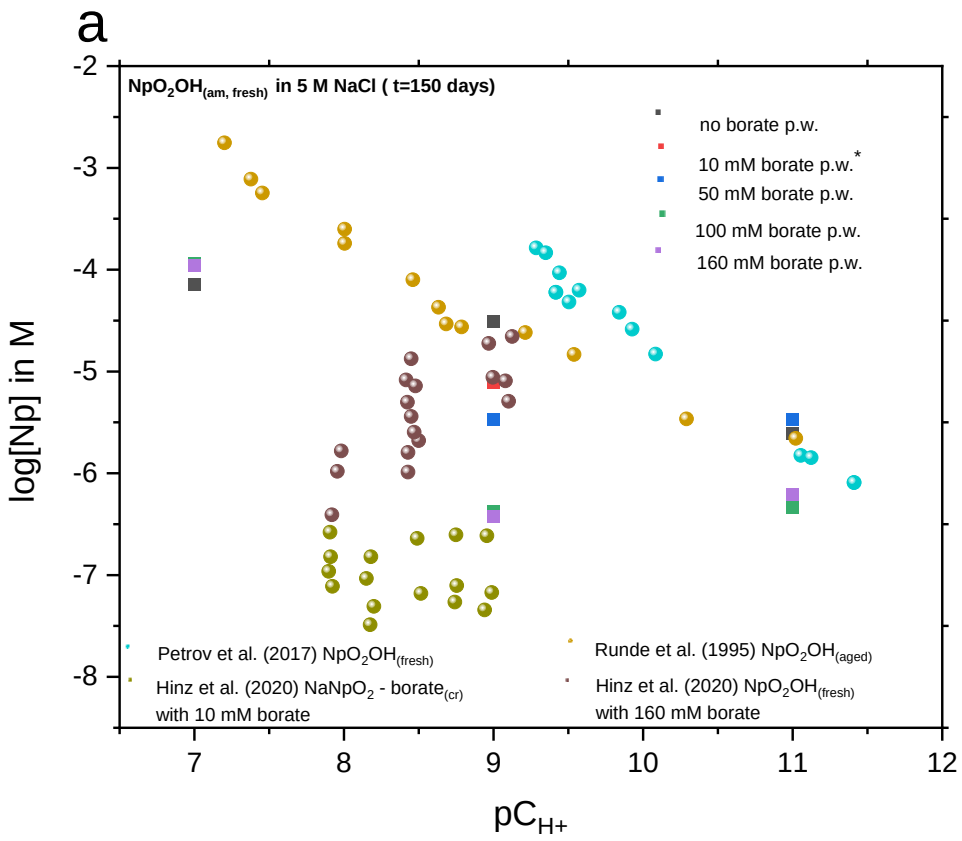

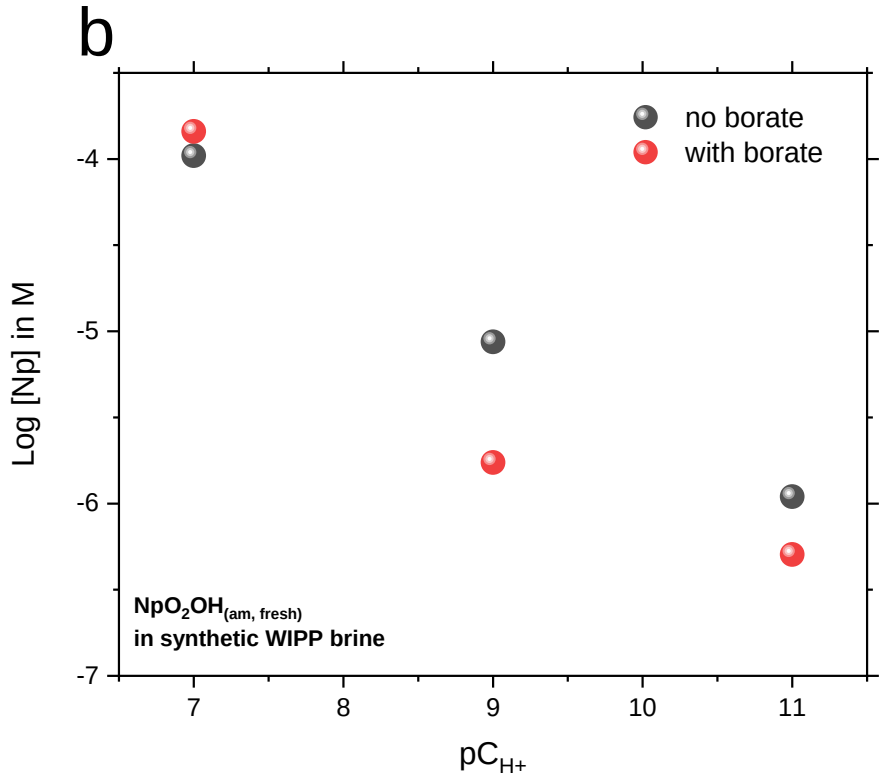

Figure 7. a) Solubility of $NpO_2(OH)_{(am, fresh)}$ in the presence of 10 mM M $\leqslant [B]_{tot} \leqslant$ 160 mM M in 5 M NaCl solutions function of pC_{H+}. Comparison with experimental solubility data in the absence and presence of borate [Petrov 2017, Runde 1995, Hinz 2020]; b) Solubility of $NpO_2(OH)_{(am, fresh)}$ in synthetic WIPP brine in the presence and absence of 160 mM M borate function of pC_{H+}.

Carbonate effect on Np solubility:

The solubility of $NpO_2(OH)_{(am)}$ was investigated as a function of pC_{H+} and carbonate concentration of 1 mM $\leqslant [CO_3^{-2}] \leqslant$ 100 mM in 5 M NaCl and 16 mM $[CO_3^{-2}]$ in synthetic WIPP brine at $pC_{H+}7$, $pC_{H+}9$ and $pC_{H+}11$ using under saturation experimental approach. This system is more complex than carbonate-free systems. NaCl solution does not have a significant pC_{H+} buffer capacity. The addition of sodium carbonate solutions, which are basic, to a 5 M NaCl solution caused a slow drift in the pC_{H+} after initial adjustment.

The samples were equilibrated over 150 days. Carbonate was added to the brine directly (i.e., not by equilibration with a carbon dioxide gas) as a spike.

The solubility of $NpO_2(OH)_{(am)}$ in 5 M NaCl at pC_{H+} 7 decrees by a very small quantity with increasing carbonate concentration. All measurements of Np concentration in the presence of various carbonate concentrations exist in a half order of magnitude lower.

No effect of carbonate on the solubility of $NpO_2(OH)_{(am)}$ in synthetic WIPP brine at pC_{H+} 7 was observed under the same conditions in the absence of carbonate.

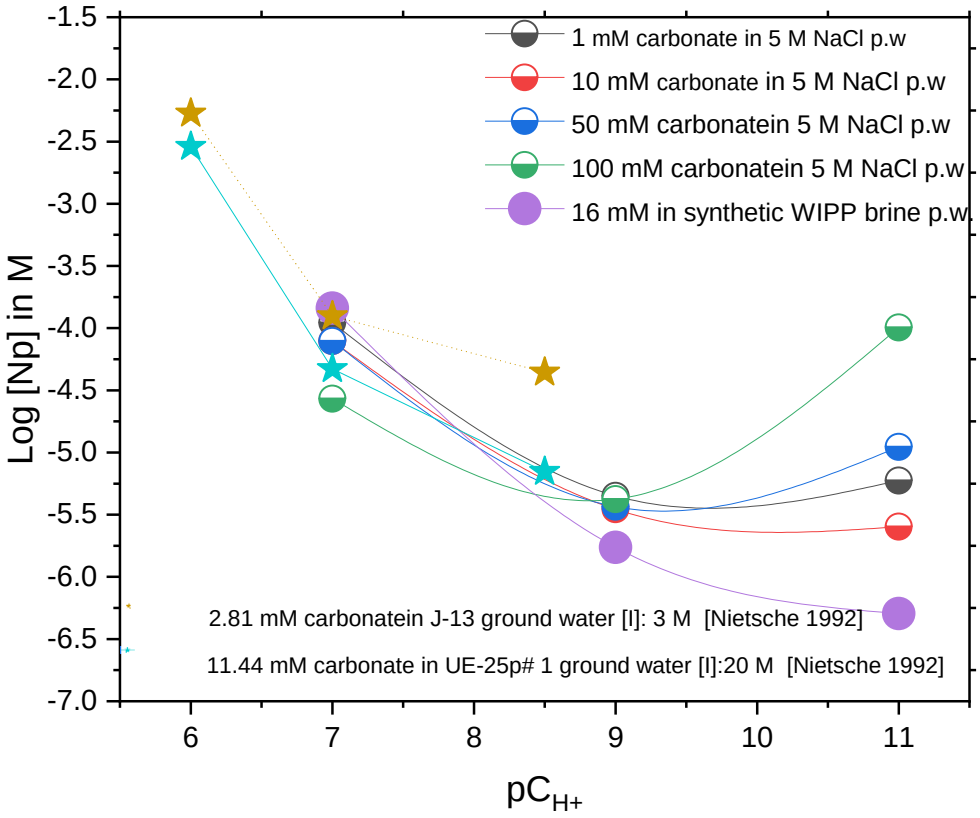

Figure 8. Solubility of $NpO_2(OH)_{(am, fresh)}$ in the presence of 1 mM M ≤ $[CO_3^{-2}]_{tot}$ ≤ 160 mM in 5 M NaCl and synthetic WIPP brine function of pC_{H+}. Comparison with experimental solubility data of Np presence of carbonate in different groundwater [Nitsche 1992].

A similar result was reported by Nitsche et al.; in two Yucca mountain groundwater with an ionic strength of 3 M at pC_{H+} 7 with $[CO_3^{-2}]$: 2.81 M and ionic strength of 20 M at pC_{H+} 6.7 with $[CO_3^{-2}]$: 11.44 M the solubility effect of carbonate on Np concentration. The solubility's of Np(V) decreased in the water with the higher carbonate content at pC_{H+} 7 and 9 [Nitsche 1992].

The Np concentration drops rapidly with all carbonate concentrations in the range of 1 mM M $\leqslant$ $[CO_3^{-2}]$ $\leqslant$ 100 mM in 5 M NaCl at pC_{H+} 9. All Np solubility results are similar to each other because of the stabilizing effect of actinide carbonate complexation reactions at about pC_{H+} 9.

The Np solubility tendency in Figure 8 show significant differences between pC_{H+} 7 - 9 and pC_{H+} 9 - 11 in 5 M NaCl. The decrease in Np concentration for $7< pC_{H+}<9$ is consistent. In contrast, increase in Np concentration for $9< pC_{H+}<11$ is consistent. This increase was due to the predominance of carbonate over hydrolysis complexation of Np in alkali condition. The pC_{H+} range of 7.5 to 10 is where carbonate effects are expected to predominate relative to hydroxide because of the pKa of carbonic acid. For higher pC_{H+}, hydroxide effects prevail over the carbonate effects. (For time depending results can be found in Figure 12 in Appendix).

Runde et al., studied solid-liquid equilibria of Np(V) presence of various carbonate concentrations in 5 M NaC1. Their results showed light on the understanding of Np speciation in the containing carbonate system. The solubility-controlling solid for both curves at low carbonate is the hydrated ternary Np(V) carbonate, $NaNpO_2CO_3 \bullet 3.5H_2O(s)$. Interestingly, this solid initially forms at high carbonate concentrations. While it is kinetically favored to precipitate, it is thermodynamically unstable. Over time, it transforms to the thermodynamically stable equilibrium phase $Na_3NpO_2(CO_3)_2 \bullet nH_2O(s)$ [Runde 2000].

6. Conclusion and Future Work

Under saturation solubility experiments with Np(V) in combination with spectroscopic investigations and a comprehensive, multimethod liquid phase characterization confirm the impact of borate, organic ligands and carbonate on the aqueous speciation and especially on the solubility of Np(V) in 5 M NaCl and WIPP brine solution on function of pC_{H+}.

The results collected within 150 days solubility experiments show that Np has not yet reached an equilibrium in all investigated condition.. It was decided to continue the experiments until the neptunium reaches equilibrium with all investigated matrix. After the equilibrium phase occurs, the new formed solid phase will be characterized using comprehensive, multimethod characterization by XRD, SEM–EDS and EXAFS.

7. Appendix

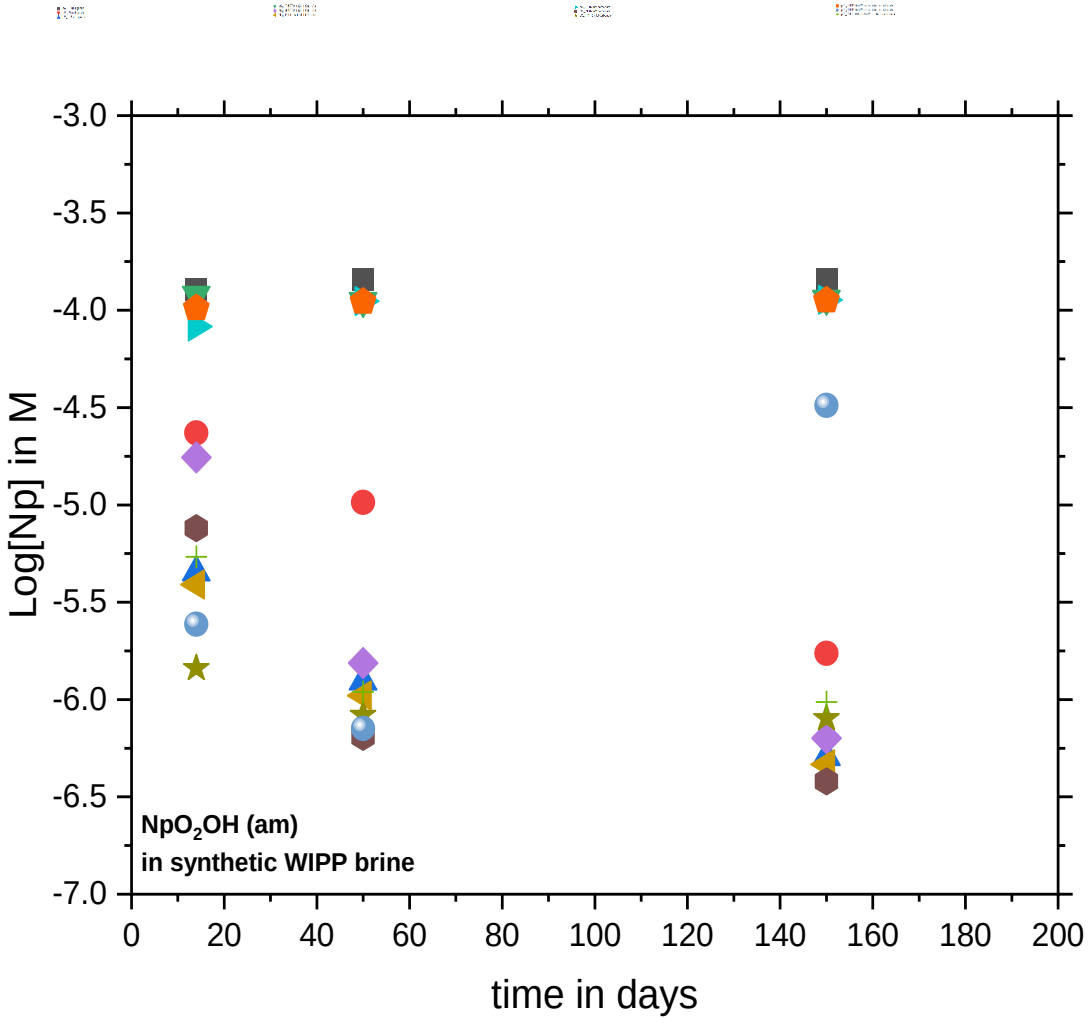

Figure 9. Solubility of $NpO_2(OH)_{(am,\ fresh)}$ in the absence and presence of (in)organic ligands "Citrate: 2.30 x 10^{-3} M, Acetate: 2.83 x 10^{-2} M, Oxalate: 1.13 x 10^{-2} M, EDTA: 7.92 x 10^{-5} M and 16 10^{-3} M Carbonate" at pC_{H+}7, pC_{H+} 9 and pC_{H+} 11 as a function of time in in synthetic WIPP brine solution.

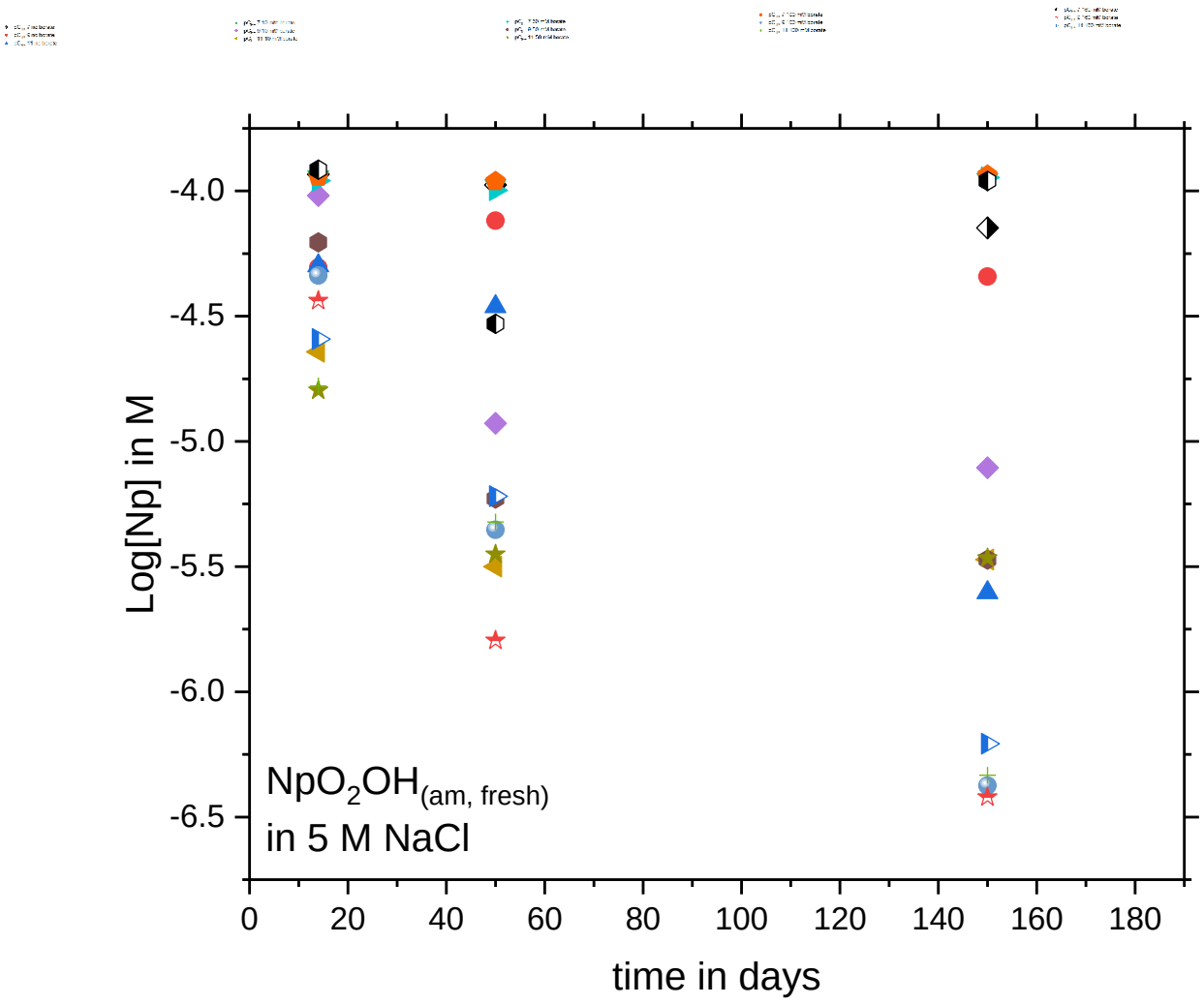

Figure 10. Solubility of $NpO_2(OH)_{(am,\ fresh)}$ in the absence and presence of 10 mM M ≤ [B]tot ≤ 160 mM at pC_{H+}7, pC_{H+} 9 and pC_{H+} 11 as a function of time in 5 M NaCl solution.

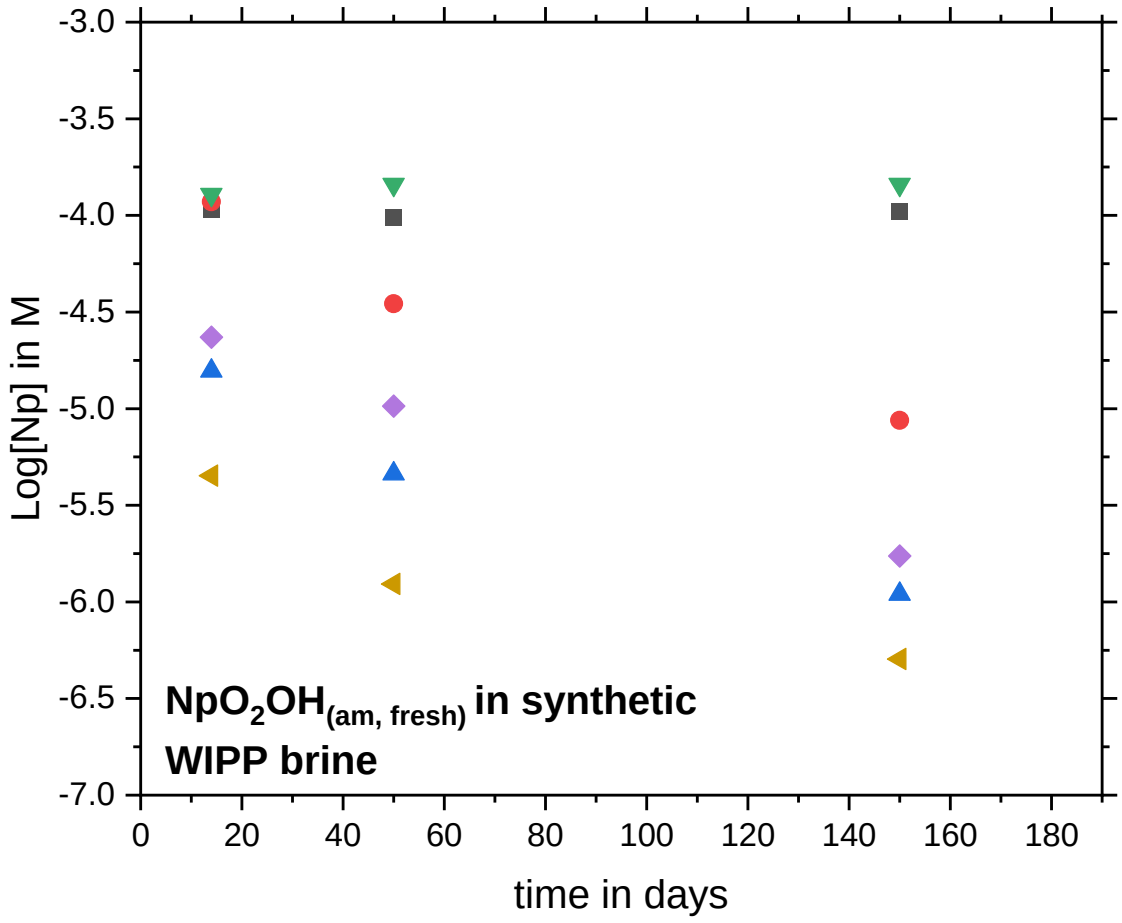

Figure 11. Solubility of $NpO_2(OH)_{(am,\ fresh)}$ in the absence and presence of borate at pC_{H+}7, pC_{H+} 9 and pC_{H+} 11 as a function of time in synthetic WIPP brine.

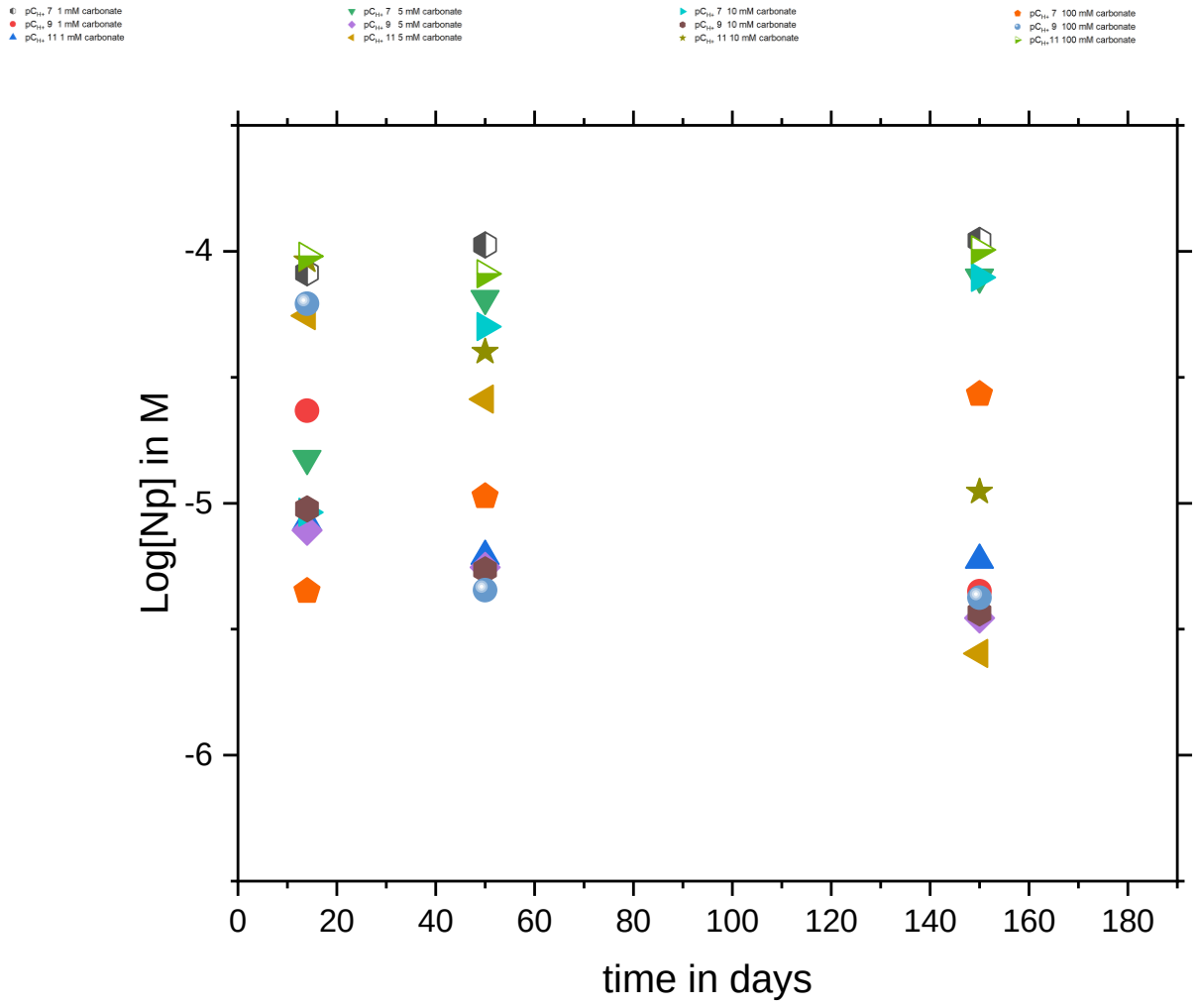

Figure 12. Solubility of $NpO_2(OH)_{(am, fresh)}$ in the presence of 1 mM M ≤ $[CO_3^{-2}]_{tot}$ ≤ 160 mM in 5 M NaCl and synthetic WIPP brine at pC_{H+}7, pC_{H+} 9 and pC_{H+} 11 as a function of time.